Advances in Energy Science and Technology

Vol. 1, No. 4| Apr 2025

AEST

Plasma-based techniques for clean and efficient hydrogen generation: A comprehensive review

Sima ealanloo [a], **Fatemeh Ahmadinouri** [a, *], **Parviz Parvin** [a]

[a] *Department of Energy Engineering and Physics, Amirkabir University of Technology (Tehran Polytechnic), Tehran, Iran.*

Keywords

Hydrogen generation
Methane reforming
Hydrocarbon conversion
Clean energy

Article Info

DOI: 10.22060/aest.2026.25852.1006

Received date: 5 March 2026

Accepted date 29 March 2026

Published date 1 April 2026

* **Corresponding author:** Parvin@aut.ac.ir

Abstract

Hydrogen is widely regarded as a promising clean energy carrier because of its high energy density and carbon-free utilization. This review presents a comprehensive overview of plasma-based techniques for hydrogen generation from water, methane, and other hydrocarbons, with emphasis on laser-induced plasma (LIP), spark discharge-assisted laser-induced plasma (SD-LIP), dielectric barrier discharge (DBD), corona discharge, microwave (MW) plasma, radio-frequency (RF) plasma, and glow/abnormal glow (GA/RGA) discharge systems. These methods provide highly reactive environments that promote molecular dissociation and hydrogen formation under relatively mild conditions. Particular attention is given to hybrid laser–spark approaches, which can enhance plasma density, prolong plasma lifetime, improve conversion efficiency, and reduce energy consumption. The review also compares the main plasma configurations in terms of operating principles, hydrogen yield, efficiency, and practical applicability. Overall, plasma-based routes show strong potential as flexible and sustainable alternatives for next-generation hydrogen generation.

Graphical Abstract

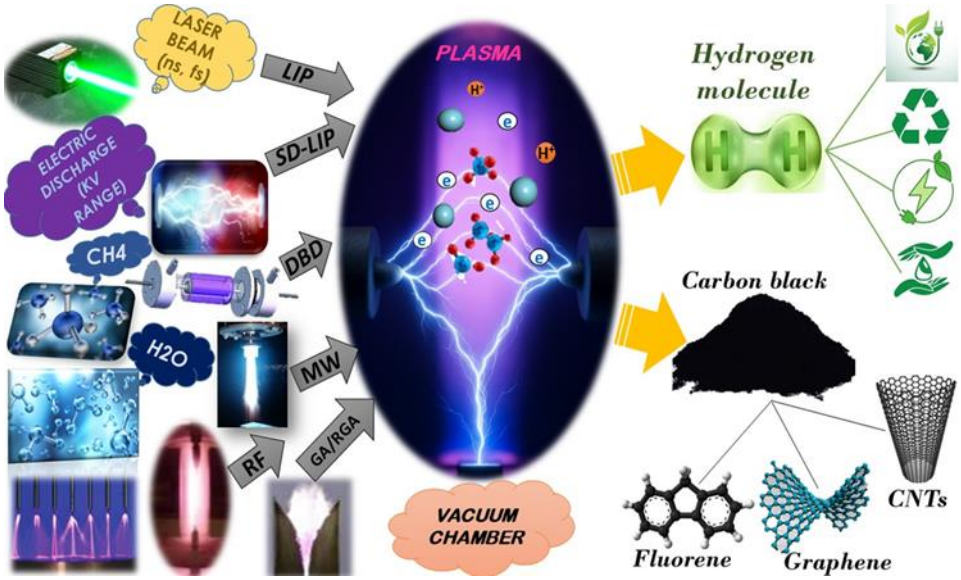

1. Introduction

The global consumption of hydrocarbons throughout the 20th century has led to severe air pollution and drastic climate change. Thus, the growing need for alternative energy sources during the recent decades has resulted in a variety of renewable initiatives. Meanwhile, hydrogen acts as a clean fuel and possesses the suitable characteristics for replacing conventional fuels in diversified energy systems [1]. The hydrogen energy offers proper prospects for fuel cells and other energetic applications. When hydrogen is combined with fuel cells effectively produces sustainable electric power. Moreover, hydrogen is utilized in many ways in petrochemical industries, such as ammonia and methanol production [2]. It shows potential for applying energy to heating and power systems as well as transportation operations. On the other hand, the hydrogen requirement is anticipated to grow substantially as a clean alternative technology in favor of mobile energy systems. The hydrogen consortium projected that the number of vehicles equipped with the hydrogen fuel cell would rise to 10 million cars as well as 500,000 trucks, in the near future [3]. Hydrogen has several key benefits, including exceptional energy conversion efficiencies, CO_2-emission-free combustion, and multiple storage options (e.g., as a gas or liquid or through metal hydrides) [4]. Currently, the annual global use of hydrogen stands at around 95 million tonnes, serving as both an energy source and a reactant in the synthesis of valuable chemicals and fuels such as gasoline, ammonia, methanol, and various other high-value products [5]. Consequently, the development of clean, efficient, and sustainable hydrogen production technologies has become a critical research priority worldwide.

Hydrogen production technologies can be fundamentally differentiated by their primary energy input mechanism. Laser-based methods employ highly coherent, monochromatic photon flux to drive localized water dissociation, photo electrochemical excitation, or laser-induced plasma reactions, enabling precise spatiotemporal control over reaction kinetics and pathway selectivity. In contrast, non-laser approaches rely on thermal gradients, applied electrical potentials, or incoherent radiation to drive bulk-phase reactions. This distinction governs critical differences in energy conversion efficiency, catalyst design requirements, operational scalability, and thermodynamic constraints, with laser-driven routes offering enhanced reaction specificity but facing challenges in continuous large-scale deployment, whereas non-laser technologies are more industrially mature but often limited by lower photon utilization or higher thermal/electrical energy demands [6]. Within the realm of light and laser methods, a further distinction can be made between discharge-based techniques and non-discharge techniques, each offering distinct mechanisms and advantages for hydrogen production. As demonstrated in recent analyses of plasma-mediated water splitting (Cook *et al.*, 2025), discharge-based approaches rely on the generation of highly ionized reaction media to drive dissociation pathways, often enabling rapid reaction kinetics and highly localized energy deposition. In contrast, non-discharge photonic methods, operate through direct photon absorption by catalyst materials without plasma formation. This fundamental dichotomy governs critical differences in reaction mechanisms, energy coupling efficiency, catalyst design requirements, and scalability potential [7].

Discharge-based light and laser methods represent a significant category of hydrogen production technologies that employ electrical discharges or laser-induced phenomena to generate reactive species capable of breaking chemical bonds in feedstock molecules. This approach builds on established principles of low-temperature plasma science, wherein energetic electrons efficiently generate radicals and excited species that drive chemical transformations [8]. Among these techniques, Laser-

Induced Plasma (LIP) has gained remarkable attention as a novel approach for hydrogen generation. Focusing the laser beam on the surface of a target leads to melting and vaporization. The particles are ejected directly from the target material (by mechanical fragmentation) as a result of laser-induced stress [9]. This is due to splashing of the molten material [10] or to explosive boiling of the target [11]. Despite the advances made in the field of plasma-catalyst, the requirements for high input power and its low energy efficiency appear to be the main obstacles to its widespread use. The input power scale-up significantly induces the undesired overheating and subsequent coking effects to deactivate the conversion performance. In addition, high-pressure performance is correlated with low spark mobility, leading to the erosion of the electrodes and finally reducing their lifetime [12]. To address the inherent limitations of conventional plasma-catalyst systems, recent studies have integrated laser-induced plasma with catalyst-spark discharge, resulting in the development of the SD-LIP technique. In this hybrid configuration, the laser functions as an insitu cleaning beam that continuously removes coke deposits, effectively preventing catalyst deactivation. Furthermore, plasma reheating is facilitated by the inverse Bremsstrahlung mechanism [13], which drives the generation of highly energetic electrons and subsequently enhances the local electron density within the reaction zone [14,15]. Ahmadinouri *et al.* explored methane conversion through a spark discharge-assisted laser-induced plasma (SD-LIP) reactor coupled with a palladium catalyst, achieving enhanced hydrogen generation efficiency. The study demonstrated that laser-triggered electron injection remarkably reduced breakdown voltage and coke formation while improving carbon balance and energy conversion efficiency. This hybrid electro-photocatalytic approach highlights the potential of SD-LIP as a promising route for clean hydrogen production from methane [16]. Ahmadinouri *et al.* also investigated hydrogen production from propane using a laser-triggered spark discharge (LTSD) system, demonstrating a substantial improvement in conversion performance over conventional plasma approaches. Their results showed enhanced hydrogen yield, markedly reduced breakdown voltage, lower energy consumption, and in situ catalyst surface cleaning that limited soot deposition and catalyst deactivation. These findings suggest that LTSD is a promising plasma-assisted route for efficient and more sustainable hydrogen generation from LPG-derived hydrocarbons [17]. Fatemeh Ahmadinouri *et al.* investigated non-oxidative methane conversion using a hybrid spark discharge-assisted laser-induced plasma (SD-LIP) system, demonstrating a significant enhancement in methane dissociation compared to conventional plasma methods. The synergistic combination reduced breakdown voltage and energy input while continuously ablating carbon soot from the catalyst surface, thereby mitigating coke formation and catalyst deactivation. The study highlights SD-LIP as an energy-efficient and controllable plasma-assisted strategy for sustainable methane conversion and hydrogen-related applications [18]. Ghasemi *et al.* demonstrated the diagnostic potential of laser-induced breakdown spectroscopy (LIBS) for distinguishing cancerous tissues from normal tissues in several human organs. Their results showed that malignant samples exhibited higher concentrations of trace elements such as Ca, Mg, and Na, along with elevated plasma temperature and electron density, indicating the formation of more energetic plasma on neoplastic tissues. The study highlights LIBS as a simple, low-cost, and real-time spectroscopic technique with promising clinical applicability for cancer diagnosis [19]. Ghorbani *et al.* studied methane decomposition in a controlled chamber using a Q-switched Nd:YAG laser, where different metal catalysts (Pd, Ni, Fe, and Cu) were ablated to form transient laser-induced plasmas over catalyst nanoparticles. FTIR and GC analyses confirmed that methane dissociates efficiently in the metal-assisted LIP, producing heavier hydrocarbons (e.g., propane, ethane, ethylene) alongside hydrogen, with product distributions strongly dependent on the catalyst and plasma characteristics. The work attributes the enhanced

decomposition to electron collisions and skin catalytic reactions on the nanoparticle surface that activate adsorption/spillover processes and loosen C–H bonds, increasing subsequent recombination pathways to higher hydrocarbons [13]. Habibpour *et al.* developed a homemade calibration-free spark-assisted LIBS (CF SA-LIBS) system for rapid gold fineness (karat) measurement. They used a Q-switched Nd:YAG laser together with a spark generator, showing that the electric discharge reheats and sustains the plasma, increasing plasma temperature (~20%), extending lifetime (~6×), and boosting signal intensity by up to an order of magnitude at low single-shot energy. Electron density was determined from broadened spectral lines and used with Saha–Eggert LTE-based relations to improve calibration-free accuracy, yielding gold karat results with <0.5% analytical error; single-shot SA-LIBS also caused less ablation/mass damage than standard LIBS, supporting portable, minimally invasive quiddity assessment [14]. Moosakhani *et al.* investigated molecular decomposition in different hydrocarbon atmospheres (C_1–C_4) by ablating a Pd target with a Q-switched Nd:YAG laser inside a controlled chamber, monitoring how the environment affects Pd ablated mass, reaction products, and plasma parameters (electron density Ne and electron temperature Te). They found that hydrocarbon media—especially methane—produce more energetic plasma than synthetic air, mainly due to oxygen-free exothermic decomposition/recombination dynamics and enhanced heating/hydrodynamic expansion from released Pd nanoparticles, which sustains plasma activity over several hundred nanoseconds. However, the same decomposition/recombination sequence also generates soot that deposits throughout the chamber, nonlinearly increasing from C_1 to C_4 and subsequently attenuating later laser shots, lowering effective plasma temperature and Pd nanoparticle population; thus, both excess exothermic heat (modestly) and soot-driven attenuation (dominantly) govern the observed differences in ablation and plasma behavior [20]. In line with exploring innovative energy technologies, the study on LIBS and LIF spectroscopy concerning crude oil-saturated carbonate bedrock, thoroughly examining its constituent elements and the thermal behavior of crude oil compounds, was conducted by Parvin *et al.* and his colleagues. This study significantly aids in the identification and differentiation of crude oil components [21]. Lethal brain cancers, such as glioblastoma multiforme (GBM) and oligodendroglioma (OG), pose significant diagnostic challenges. Laser-induced breakdown spectroscopy (LIBS) offers a promising avenue for minimally invasive diagnosis by analyzing plasma emissions from tissue samples. In recent work by mohammadimatin *et al.*, advancements like spark-assisted LIBS (SA-LIBS), have demonstrated a remarkable enhancement in spectral signals and plasma properties (temperature, electron density, ionization) compared to conventional LIBS. This technique shows a notable ability to discriminate between cancerous glioma lesions and infiltrated healthy tissues, with enhanced ionic emissions from species like Mg II and Ca II serving as key indicators for early-stage cancer grading [22].

Corona discharge represents another important discharge-based technique which is characterized by the formation of a self-sustained plasma around a sharp electrode tip when a high voltage is applied [23]. Corona discharges operate at atmospheric pressure under non equilibrium conditions; wherein energetic electrons drive chemical transformations while the bulk gas remains near ambient temperature [24]. Corona discharge has been investigated as a non-thermal plasma method for hydrogen generation from various feed stocks, including water vapor, dimethyl ether, and methane, with reported energy efficiencies ranging from ~8% for liquid-water systems to nearly 80% when steam and argon carrier gas are employed [25]. Microwave (*MW*) plasma systems generate discharges by coupling electromagnetic radiation in the gigahertz frequency range (typically 2.45 *GHz*) into a gaseous medium, enabling stable, electrodeless operation. A defining advantage of this configuration is the

highly uniform spatial distribution of energy deposition across the plasma volume, which minimizes thermal gradients and promotes consistent reaction environments. Additionally, *MW* discharges provide exceptional tunability of key plasma parameters, as electron density, gas temperature, and power coupling can be independently optimized by adjusting input power, operating pressure, gas flow rate, and waveguide or cavity geometry [26]. Jasiński *et al.* [27–30] investigated atmospheric-pressure microwave plasma for hydrogen production via methane decomposition and reforming using pure CH_4 and CH_4/gas mixtures. Their studies demonstrated that this configuration achieves high methane conversion and competitive hydrogen energy yields without requiring external catalysts or high-temperature reactors, positioning atmospheric MW plasma as a highly efficient alternative to other discharge-based techniques such as gliding arcs, plasmatrons, and electron-beam systems. In the work by Czylkowski *et al.* [31], a combined steam reforming in microwave plasma technology for hydrogen production in CH_4/CO_2 was used for the first time. They obtained an energy yield of hydrogen production of $43 g(H_2)/kWh$, which is not far from the US Department of Energy's energy yield requirement ($60 g(H_2)/kWh$).

Radio Frequency (RF) discharge technology operates at frequencies typically between 1 *MHz* and 100 *MHz*, generating plasma through oscillating electric fields that accelerate electrons to sustain ionization while maintaining low bulk gas temperatures [32]. RF plasmas are characterized by their ability to produce large-volume, uniform plasmas with low gas temperatures due to the non-equilibrium state where electron temperatures greatly exceed neutral gas temperatures ($T_e \gg Tgas$), making them attractive for hydrogen production from various carbon-containing feedstocks [33].

The discovery of ozone was about 20 years earlier, in 1839, by Christian Friedrich Schönbein. Siemens developed a highly transient and localized nonthermal plasma at atmospheric pressure, and called it a "silent discharge", which is currently known as a dielectric barrier discharge (DBD) [34]. DBD has attracted a special attention, due to its advantages, such as the ability to produce a wide array of chemically reactive species under ambient conditions, uniform distribution of the discharge, high electron density etc. [35].

Gliding arc discharges provide an easily controllable energy source that enables substitution of high-temperature thermal processes with lower-energy cold plasma processes for engineering and environmental applications [36]. The gliding arc in tornado (GAT) configuration incorporates a tangential reverse vortex flow that forces the arc to rotate around the cylindrical reactor axis, ensuring more uniform gas treatment and significantly larger residence time for reacting species compared to conventional flat-geometry gliding arc systems [37]. RGA plasma is considered a warm plasma that has both thermal and non-thermal properties, indicating a relatively high electron density and electron energy as well as moderate gas temperature, which is beneficial for hydrogen production and high productivity [38], and has been used by some authors to produce hydrogen from methane reforming [39-41].

Natural gas, which is primarily methane, is the predominant source for H_2 production commercially due to its abundant reserves and high H/C ratio. In an oxidative methane reforming process, methane and an oxidant such as H_2O, O_2, and/or CO_2 are initially cofed with or without the assistance of a catalyst to produce syngas. These processes are normally operated at high temperatures (700−1300°C) due to the endothermic nature of the reactions (e.g., methane steam reforming and methane dry reforming with CO_2). The water-gas shift reaction enhances the H_2 production yield and converts CO to CO_2 [42]. Early studies on plasma-assisted oxidative methane reforming can be traced back to 1897, which predates the formal definition of "plasma" by Langmuir [43,44]. Non-oxidative conversion of CH_4 is considered a promising route for the generation of H_2; however,

most efforts in this area have focused on the production of higher hydrocarbons as valuable fuels and chemicals, with H_2 as a byproduct. Although the selective production of H_2 is not often targeted in non-oxidative CH_4 reforming processes, H_2 remains a valuable product and processes could be re-evaluated with the focus of improving H_2 yields. Direct conversion of CH_4 is an attractive alternative for the production of fuels and chemicals. Many efforts have been made to advance this chemistry, including approaches such as thermal, homogeneous/heterogeneous catalysis, photo-catalysis, electro-catalysis, and plasma-catalysis [45].

Alongside the development of novel hydrogen generation methods, overcoming the challenges in hydrogen storage is key to unlock its full potential as a clean energy carrier. Mortazavi *et al.* reported a one-step laser-assisted route for decorating multi-walled carbon nanotubes (MWCNTs) with palladium nanoparticles, enabling modification of the nanotube surface for hydrogen storage. Their results indicate that Pd decoration improves hydrogen uptake compared with pristine MWCNTs, while the laser exposure exhibits an optimal range beyond which storage performance can degrade due to irradiation-induced damage [46]. Mehrabi *et al.* propose a hybrid method combining laser ablation and chemical reduction to decorate multi-walled carbon nanotubes (MWCNTs) with metal nanoparticles (Pd and Ni), increasing nanoparticle loading and creating additional nano-cavities that enlarge the effective surface area. Structural and porosity analyses (TEM, XRD, thermal/elemental methods, BET, BJH) confirm controllable nanoparticle characteristics and morphology, while volumetric measurements show enhanced hydrogen storage. Hydrogen uptake reaches 8.6% for Pd-decorated MWCNTs and 2.5% for Ni-decorated MWCNTs (at higher Pd and lower Ni optimal metal populations), explained by hydrogen spillover and associated trapping, with a competing pore blockage effect at excessive metal loading [47]. In another work Mehrabi *et al.* examine how nickel nanoparticle decoration (via laser ablation/chemical reduction) affects hydrogen storage in MWCNTs using volumetric hydrogen sorption/desorption measurements. They find that hydrogen uptake increases with higher Ni population up to an optimum, but then drops at excessive Ni, attributed to laser-induced changes in pore size/volume (which reduce hydrogen trapping) and to pore blockage/hindered diffusion when Ni loading becomes too high; the laser-treated samples also show more efficient trapping overall. The best storage is reported at about ~1% (0.6 *wt%*) hydrogen for Ni-MWCNTs with ~12.3% (13 *wt%*) Ni loading (depending on method), alongside a lower desorption temperature and improved plateau/cycling behavior for Ni-MWCNTs (and they also note Ni's lower cost vs Pd and that laser treatment reduces differences between Ni and Pd systems) [48].

This review article offers a broad overview of plasma-assisted hydrogen production methods, with a special focus on discharge-based light and laser techniques such as LIP, SD-LIP, corona discharge, microwave, RF, DBD, and gliding arc systems. It examines the basic mechanisms, reactor designs, performance features, and recent developments in each technology in a critical way. In addition, the comparison between oxidative and non-oxidative plasma methods helps explain why non-oxidative approaches are becoming increasingly preferred for hydrogen production. The article also discusses the main challenges, opportunities, and future directions of plasma-based hydrogen production technologies to support researchers and practitioners in this fast-growing field.

2. Overview of plasma discharge types for hydrogen generation

2.1. Laser-Induced Plasmas

2.1.1. Laser-Induced Plasma (LIP)

Early experimental investigations of laser-induced plasma formation emerged in the years following the invention of the ruby laser, focusing on fundamental plasma physics, particle emission, and laser–material interactions [49]. Shortly after the pulsed ruby laser was invented in 1960, laser-induced plasma was observed. The first published report mentioning the plasma as a spectral source was a meeting abstract by Brech and Cross in 1962, and the first analytical application of LIBS (laser-induced breakdown spectroscopy) for surface spectrochemistry appeared in 1963 (Debras-Guédon & Liodec). Systematic development of LIBS methodology accelerated in the late 1970s through research at Los Alamos National Laboratory [50].

Laser-induced plasma (LIP) is generally assumed to be optically thin regarding Local Thermodynamic Equilibrium (LTE), emphasizing that collisional processes dominate over radiative ones [19]. The laser induced plasma emission relies on the electron impact excitation events, while the photo-excitation process shows a minor contribution [51]. The extra populations of the excitation states resemble further the enhancement of characteristic emission. On the other hand, the extra initial electrons give rise the relatively larger plasma volume in the same conditions [52].

By making use of the metal targets, the laser energy required for the breakdown is significantly reduced due to the higher electron density and electron mobility of the metallic target [53].

ablation generally occurs during laser-induced plasma due to the driving force of the laser and its thermal effect (i.e., Inverse Bremsstrahlung [IB] process). The ablation can also take place after the laser pulse duration due to the hydrodynamic forces of the plasma expansion [20].

A focused pulsed laser beam on the target results in the rapid temperature rise (>1011 *K/s*), with maintenance of the stoichiometry of the nanoparticles. High-energy atoms and ions in the laser-induced plasma plume create a high surface mobility which accounts for nanoparticles' generation. During the laser beam interaction with the target surface material, there are various processes leading to atoms and clusters and droplet expulsion from the target surface. The most common case is the nanoparticle production by the pulsed laser ablation [54−56]. The method involves the condensation of atoms/molecules and cluster formation (with or without any chemical reactions) during the fast expansion of the vapor/ plasma plume generated in front of a target. The time of nucleation and size and composition of clusters depend on the type of material, the laser parameters, and the ambient medium [57].

The electron energy distribution of laser-induced plasma spreads over a few electron volts. Hence, the multiple electron impact collisions may dissociate or ionize the molecules. Furthermore, the utilization of metallic catalyst drastically decreases the electron energy that is required for the methane decomposition. The non-Maxwellian electron energy distribution of laser-induced plasma is typically ranging 1−5 *eV* while the threshold energy for dissociation requires greater than 9 *eV*. Hence, the plasma seldom dissociates methane by itself [58].

Material ablated into the plasma may be in the form of particles (either fresh, or melted and cooled) as well as atoms and/or molecules. In fact, laser ablation is governed by a variety of distinct nonlinear mechanisms. Once the laser beam illuminates the sample, the mass leaves the surface in the form of electrons, ions, atoms, molecules, clusters, and particles, each of the

processes separated in time and space [59,60]. However, during methane decomposition in plasma, the ablated catalysts are mostly metal NPs such that methane molecules can attach to them, with subsequent catalysis of the decomposition to CH_2 and then recombination to higher compounds [61,62].

The decomposition of various hydrocarbon molecules has been extensively investigated in the literature. The first paper using laser induced plasma on the surface of metallic target to initiate chemical reactions of hydrocarbons was published in 1979 [63,64]. The authors focused a TEA-CO_2 laser beam on the metallic surfaces such as Pb, Ni, and W in the methane atmosphere leading to acetylene and molecular hydrogen generation. The first laser-plasma assisted heterogeneous catalytic process was reported to decompose methane at the oxide surface namely Li/MgO [65].

laser ablation technique in liquid provides an effective means to synthesize nanoparticles. One of the main characteristics of laser-induced plasma inside liquids is fast quenching due to a dense medium. When a nanosecond pulsed laser with sufficiently high energy density strikes the interface between liquid and the metal target, it forms a micro plasma layer after a series of sequential events. At first, the laser beam is absorbed by a metallic target to create a molten layer, and then further absorption leads to the local rise in temperature up to the boiling point of the metal, where several physical phenomena such as fragmentation, sublimation, and atomization occur simultaneously [60, 66, 67].

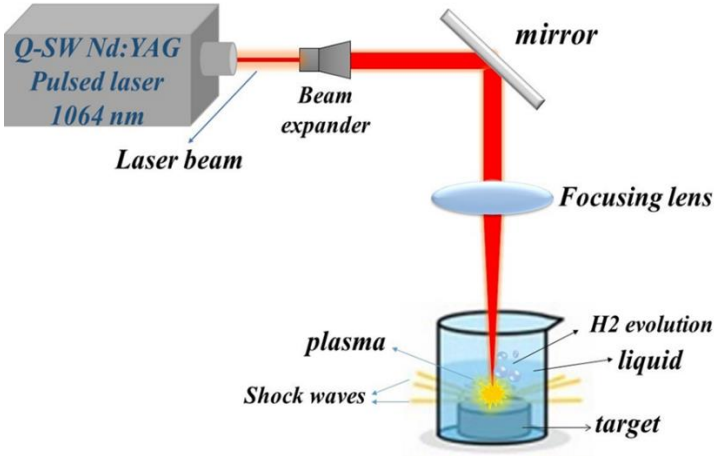

Fig. 1. Schematic of the Laser-Induced Plasma (LIP) setup for hydrogen generation, showing laser focusing on a target in liquid to produce plasma, shock waves, and H_2 evolution.

Advances in Energy Science and Technology
Vol. 1, No. 4| Apr 2025
AEST

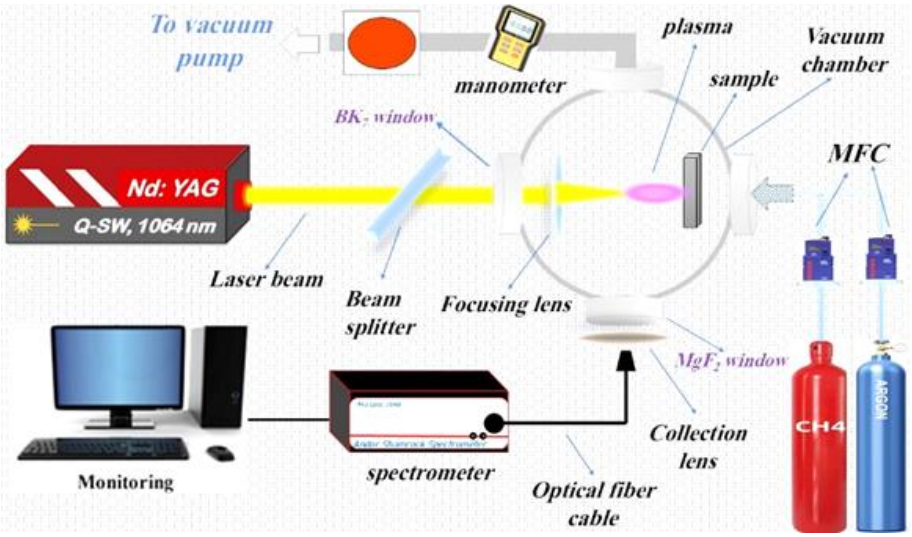

Fig. 2. Laser-induced plasma setup showing laser delivery, focusing optics, vacuum chamber with controlled Ar/CH_4 atmosphere, and plasma emission collection. The system enables precise control of pressure and gas flow for LIP generation and spectroscopic diagnostics.

2.1.2. Spark-Discharge Laser-Induced Plasma (SD-LIP)

Tremendous efforts have been made on the cold plasma, i.e., corona discharge (CD) [68,69], dielectric barrier discharge (DBD) [70,71], as well as warm plasma including the gliding arc discharge (GAD) [39,72], spark discharge (SD) [73,74], microwave (MW) [75,76], and radio-frequency (RF) discharge [77] to achieve the ever-highest energy efficiency. Herein, the cold plasma techniques offer low-efficiency conversion, whereas the warm ones give rise to high gas temperatures, electron density, and electron energy to gain the most efficient decomposition events. Meanwhile, the drastic overheating effect causes the coking process to preclude vital reactions and eventually terminates the methane conversion [78]. Furthermore, the complexity of power sources in hot plasma (RF and MW) notably increases the equipment cost to restrict the system's scale-up. As a consequence, the spark discharge utilization can be optimal during the warm plasma mode, especially in direct combination with a solid catalyst. In actuality, the successive discharge pulses prevent heating, allowing switch-off cycles among the continuous discharge intervals to level down the overheating effects [74,79,80].

In spark discharges (SD), a typical set-up consists of two electrodes connected to a charged capacitance [81]. When high enough voltage V_0 is applied, a so-called streamer is formed first. Once it reaches the opposite electrode, plasma breakdown takes place, followed by the streamer transition to an expanding plasma column. In this column, Joule heating of both plasma and electrodes take place. In addition, electrodes are bombarded by energetic ions that induce sputtering, which can be considered to be similar to laser ablation. If background gas is present, rapid thermalization of the sputtered material leads to primary nanoparticle formation that can then grow by collisions and form larger particles or aggregates.

For spark discharge, when gas density decreases, plasma resistivity drops down, thus preventing further energy absorption from the electric current. During the expansion, plasma cools down and gas goes back to the axis. These processes are repeated when the energy absorption is high enough for efficient expansion [82].

When a streamer is able to connect two electrodes, without the presence of a pulsed power supply (see corona discharge above) or the presence of a dielectric (see DBD), a spark discharge can develop by further growth of the current [83].

Note that the breakdown voltage in SD is a function of the gas pressure and the electrodes gap according to Paschen's law [84]. On the other hand, the laser significantly reduces the breakdown voltage compared to spark discharge by itself through the process of inverse bremsstrahlung by improving the electron density [16]. This allows the spark discharge to take place in favor of a 6 mm electrode gap at lower voltages. It is worth noting that this characteristic significantly mitigates electrode corrosion, which is a major challenge in industrial applications [12].

Fortunately, in the SD-LIP configuration, the synergy of spark discharge coupled with laser-induced plasma would remarkably intensify the electric field, raising the mean electron energy and electron density due to the inverse Bremsstrahlung mechanism. This promotes collision rates between methane molecules and electrons, which in turn improves the rate of ECE and hydrogen production by enhancing energy-impact processes and minimizing energy loss pathways. Despite the fact that the spark discharge can generate more heat than the hybrid mode of SD-LIP, a smaller electron density appears in plasma. The findings highlight the fact that the SD-LIP technique could generate a higher electron density than a single spark discharge which makes it more effective in the course of recombination events. As a result, the rate of recombination elevates in SD-LIP, accompanying the smaller plasma temperature compared to those in SD mode. In actuality, energy contributes to converting methane rather than causing the temperature to rise [16].

In spark assisted LIBS (SA-LIBS), the electrical discharge improves the relative signal intensity ratio by reheating the plasma and increasing its lifetime [85]. Furthermore, a variety of spark discharges with customized circuits are utilized, having different electrode arrangements [86–88]

the formation of massive coke deposits and the consequent blockage of the active metal catalyst surface lead to rapid catalyst deactivation. The optimal conditions for analyzing the balanced interaction among the energy efficiency, degree of reactant conversion, and coking process are known as the main challenges of CH_4 non-oxidation conversion. According to our findings, an elaborate combination of solid catalyst and spark discharge accompanying the laser-induced plasma treatment gives rise to an effective suppression of coke formation [16]. Note that the hybrid SD-LIP enables us to clean the catalyst surface effectively after each laser shot by ablating the carbon soot (coke) residues to slow down the rapid catalyst deactivation. Hence, in principle, laser function synergeticly facilitates the controlled discharge ignition and the coke ablation. In fact, the electrical spark discharge does enhance the system power because it is more accessible and economical than that of LIP to decompose methane in terms of the applied energy. As a consequence, not only combination of the hybrid laser-induced plasma and spark discharge could elevate the efficiency, but also notably promotes its controllability. This feature is particularly helpful in applications where system reliability and enhanced performance are essential such as on-board transportation or the miniatured petrochemical operations [18].

the LTSD (Laser-Triggered Spark Discharge) technique combines the simpler operation and pulsed power benefit of spark discharge with the accuracy, electron management, and self-cleansing ability of laser plasmas. Application of this hybrid system would eliminate the energy inefficiency, coking, and pressure challenges that annoy conventional SD systems and can provide a selective, efficient, and robust platform to produce hydrogen from hydrocarbon sources such as propane. It should be noted that traditional methods often result in making much more carbon dioxide than hydrogen as a by-product. The main benefit of the LTSD method is that it allows propane to be converted non-oxidatively, so hydrogen is produced from propane directly without creating carbon dioxide. This process makes it possible to convert hydrocarbon gases into

clean hydrogen fuel without releasing greenhouse gases. This decarbonization is very important for the environment and energy sustainability.

In the LTSD approach, the energy conversion can be significantly increased by raising the spark voltage, laser energy, and number of shots. Besides other factors, the amount of reactor volume is important for conversion efficiency and has to be included in assessing various systems.

Setting aside the unique advantage of this process, the potential weakness of the method includes: (i) Expensive laser system; however, using advanced technology, this equipment has gradually become more inexpensive in the recent decade. (ii) At the moment, the efficiency of the method can be promoted to raise its attraction from low-scale units in the industry, which can be improved using hybrid catalysts and intense laser shots/spark discharge in large-scale applications [17].

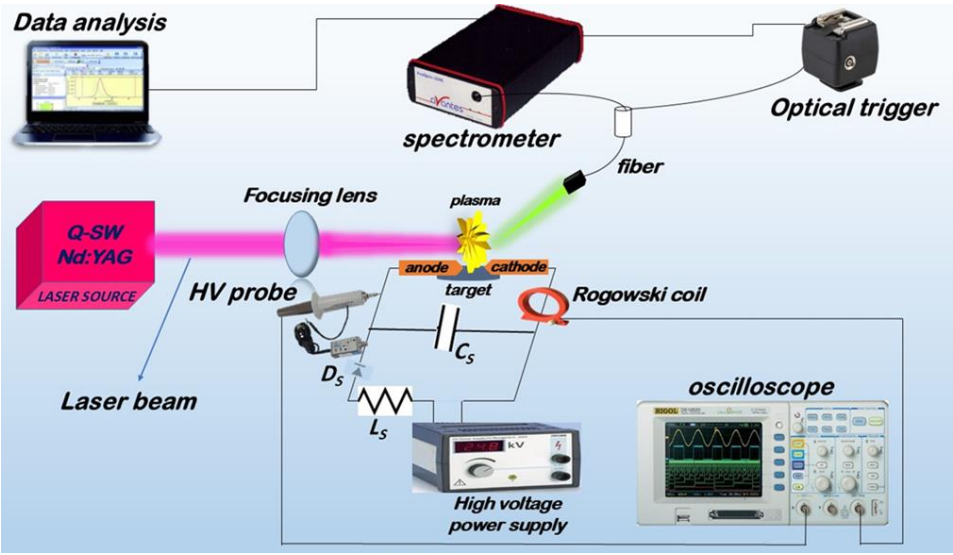

Fig. 3. Experimental configuration of the SD-LIP technique, highlighting the optical path and the integrated diagnostic tools (spectrometer, Rogowski coil, and oscilloscope) used for characterizing the ablation process.

2.2. Electrical Discharge Plasmas

2.2.1. Dielectric Barrier Discharge (DBD)

Dielectric barrier discharge (DBD) plasma is the most commonly employed method of nonthermal plasma generation in research applications. The widespread use of DBDs is attributed to the ease in setup/design, ambient conditions for operation, and ability for intermittent start-up and shutdown operations [89-91]. DBDs are constructed with one or more layers of insulating (dielectric) material located between two electrodes that are connected to an electric power source [91-93]. Typically, the DBD plasma is formed in either planar or coaxial configurations [91]. The dielectric thickness is usually on the order of a few millimeters and made of materials such as quartz, glass, polymers, or ceramics [94]. The electrode thickness is on the order of tens of micrometers [95], while the discharge gaps can vary from a few millimeters to centimeters, depending on the application [96]. Upon the application of high voltage, the gas in the gap between the electrodes breaks down to form a plasma while the dielectric prevents transition to an electric arc or spark discharge [97,98]. Consequently, DBD plasmas are often referred to as silent discharge plasmas due to the lack of complete gas break down [89]. The self-

limiting nature of the DBD plasma leads to the formation of filaments with an extinction time on the order of 10^{-7}s and is characterized by high local electron densities up to 10^{15} cm^{-3}[98]. Furthermore, depending on the operating conditions (frequency, voltage, gas type, temperature), discharges in the DBD plasma could be filamentary or diffuse [96]. DBD plasma experiments are typically conducted at low temperatures and atmospheric pressures. In most cases, the DBD plasma is powered by an alternating current (AC), which typically operates in a frequency range of kHz [92,94]. However, more recent applications have employed pulsed or radio frequency plasma with frequency in the MHz range [92]. At such high-frequency ranges, the gas breakdown voltage is decreased [99], and the charges are stored in the gap rather than charging up the dielectric [92]. DBD plasma has been mostly used for many plasma-catalysis studies [100].

in a DBD reactor, increasing the discharge power generally increases the number of micro discharge filaments, thus creating additional reaction pathways for chemical processes [101,102]. The discharge power is determined by the number of streamers generated per unit area and unit time; a typical number density of streamers in air DBD is 10^{6} cm^{-2} s^{-1}[103].

Dielectric barrier discharge (DBD) stands out as the predominant plasma type, especially for POX and DRM processes [104]. DBDs have advantages such as low operating temperature, compact design, ease in construction, ease in incorporating catalysts, and ability of handling various feedstocks. The electrode type [105], dielectric constant of the packed material [106-109], dielectric and reactor geometry [110-113] have a direct impact on plasma-assisted oxidative methane reforming. DBD-assisted H_2 production processes generally have an energy efficiency of 6−10% with a H_2 yield of 30−40%. Li *et al.* [105] reported that a Ti electrode exhibited the highest CH_4 conversion compared to Al, Fe, and Cu, in a DBD plasma-assisted DRM. Khoja *et al.* [104] found that the optimal discharge gap and discharge length were 3 and 300 mm, respectively, when the discharge gap was varied between 1 and 5 mm and the discharge length was varied between 100 and 300 mm in a cylindrical DBD reactor. Wang and co-workers [104,110] developed a multistage DBD reactor with a series of tandem ground electrodes sharing one high voltage electrode. The authors found that the multistage DBD reactor promoted H_2 selectivity compared to a conventional one-stage DBD reactor [110]. The authors proposed that the improvement in H_2 selectivity was due to the quenching sections between the ground electrodes, limiting CO_2 recombination [110].

Moreover, it is reported in the literature that by combining a DBD with a catalyst, in so-called plasma catalysis, the selectivity of the process can be steered towards the desired products [114-116].

In general, in terms of practical use, a DBD has some benefits compared to the other plasma types (microwave and gliding arc) because its construction is simple, robust, and allows an easy scale-up, as was demonstrated 150 years ago for the commercial application of O_3 production [83,117].

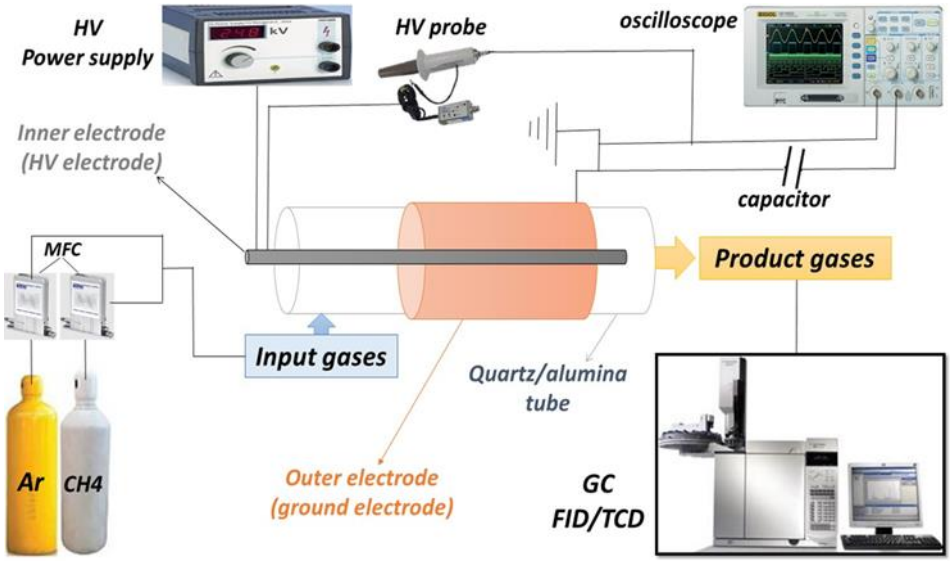

Fig. 4. Schematic of a dielectric barrier discharge (DBD) plasma reactor for hydrogen production through methane reforming, comprising a coaxial quartz/alumina tube with an inner high-voltage electrode and outer grounded electrode, mass flow controller-regulated Ar/CH_4 feed gases, gas chromatography analysis of products via FID/TCD detectors, and electrical characterization using an HV probe, oscilloscope, and capacitor.

2.2.2. Corona Discharge

Corona discharge gets its name because it resembles a crown [23]. Corona discharge is a relatively low power electrical discharge, and it is usually nonuniform, characterized by a high electric field, a relatively low current density, and strong luminosity located close to one electrode [118]. This partial self-sustaining gas discharge can be generated in a nonhomogeneous but sufficiently high electric field powered by alternating current (AC) or continuous/pulsed direct current (DC) at atmospheric pressure. Electrodes in these systems are commonly configured in several ways. As shown in **Fig. 5**, one typical setup involves a grounded plate outer electrode, complemented by a concentric high-voltage wire or rod acting as the inner electrode [119]. Alternatively, they may be arranged in point to-point or point-to-cylindrical electrode configurations. The use of asymmetrical electrodes efficiently improves the stability of the corona discharge while reducing the plasma volume. Generally, corona discharge occurs in regions of high electric field strength near sharp points, edges, or thin wires where the radius of the curvature of the electrode is small. The formation mechanism of corona discharges differs when the polarities of the electrodes are different, which lead to various discharge forms, such as positive corona, negative corona, bipolar corona, AC corona, and high-frequency (HF) corona. DC and pulsed DC reactors offer the flexibility to be operated with either polarity, while AC reactors inherently exhibit no polarity effects [23]. Additionally, a positive corona can be generated when the high electric field is concentrated around the anode, which can readily transition into spark discharges due to the high applied voltage. A negative corona is created when the high electric field is centered on the cathode, characterized by a more stable discharge behavior but a restricted operating voltage range [23].

Compared to plasma-assisted SMR and POX processes, corona systems are more commonly used in DRM. Corona discharges present an energy efficiency of ~10.7% and a H_2 yield of ~56%. Previous research has revealed that positive corona

discharges yield enhanced gas conversions in the plasma DRM reaction compared to negative corona discharges. This is attributed to the large active volume and high electron energy associated with positive corona discharges. However, the utilization of negative corona discharge proves advantageous in enhancing H_2 leading to the attainment of a H_2/CO ratio surpassing that achieved through positive corona discharge [120]. Li *et al.* [121] also observed that an increase in CH_4 conversion in different corona discharges followed the order of positive corona > AC corona > negative corona. High CH_4 conversion (70%), H_2 yield (70%), and energy efficiency (14.3%) were also achieved by using a positive corona discharge for the DRM process at a SEI of 45 kJ/L. Notably, the authors revealed a contrasting pattern in terms of the impact of different corona discharges on the H_2/CO ratio in the syngas: negative corona > AC corona > positive corona.

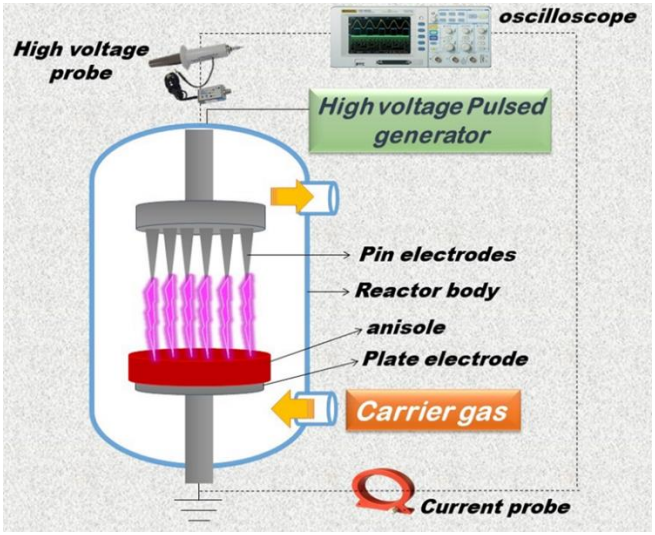

Fig. 5. A typical point-to-plane pulsed corona discharge reactor [119].

2.2.3. Gliding Arc / Rotating Gliding Arc (GA/RGA)

Gliding arc (GA) discharges are a prevalent form of warm plasmas and have a higher bulk gas temperature and current density than corona discharges or DBDs. GA discharges exhibit higher energy efficiency and high gas volume treatment capacity. The most widely used GA is the quasi-two-dimensional discharge reactor, which is composed of two or more diverging metallic electrodes (see **Fig. 6.a**) [122]. Generally, torch-like arcs are created between knife-shaped electrodes powered by DC or AC. Specifically, the ignition of the initial arc occurs at the narrowest interelectrode gap, situated between two flat diverging electrodes. This initial arc is then driven by gas flow to a larger interelectrode distance. At the same time, with the expansion of the plasma column, the gas temperature experiences a rapid drop, while the electron temperature remains high. This leads to a quick transition (on the order of nanoseconds) from thermal to nonthermal ionization that constitutes approximately 75−80% of the discharge energy [123-125]. As the interelectrode distance increases, the discharge extinguishes, and a new arc at the shortest interelectrode distance ignites once again. Consequently, high feed flow rates are necessary to maintain the arc evolution and discharge stability during the GA discharge. However, the primary challenges in conventional GA reactors involve addressing the low gas conversions caused by the short residence time of the reactants and electrode deterioration due to the carbon deposition on the electrode surface [126-127]. Various studies have reported rotating gliding arcs (RGAs) to address these issues [4]. In recent studies, advancements have been made in the development of

rotating gliding arc (RGA) reactors to increase the residence time of the reactants passing through the plasma column. Zhu and co-workers [128] developed a novel RGA reactor co-driven by a tangential gas flow and a magnetic field. With the combined effects of swirling flow and the Lorentz force, the arc can rotate rapidly and steadily around an inner cone-shaped electrode, providing a stable and large three-dimensional plasma region with an enlarged residence time of the reactants. A CH_4 conversion of 58.5% and H_2 yield of 20.7% were achieved with a 10wt%Ni/γ-Al_2O_3 catalyst packed downstream of the RGA reactor [128]. Furthermore, Lu *et al.* investigated the effect of electrode geometry (such as internal electrode summit angle and external electrode length) on DRM in a spiral feeding-gas RGA (**Fig. 6.b**). The authors found that a summit angle of 45° showed the highest CH_4 conversion (28%) and H_2 production yield (16%). This is due to the optimal balance between the sliding space and the rotating time of the arc at the top of the electrode. Additionally, a long external electrode enhanced the arc extension, increasing CH_4 conversion by 27%, compared to a short external electrode [129]. Furthermore, apart from modifying the electrode configuration, a 3D nozzle [130] and a water-cooled quenching rod [131] were also developed. These innovations have led to enhanced hydrogen production and increased energy efficiency. The former study attributed these improvements to reduced heat dissipation facilitated by the incorporation of flow-induced thermal insulation [130], while the latter investigation highlighted the suppression of the reverse water-gas shift (RWGS) reaction, which consumes H_2, aided by the introduction of a quenching device [131]. In contrast to other nonthermal plasma reforming systems, gliding arcs are able to operate with low specific power consumption and thus achieve relatively high energy efficiency [132].

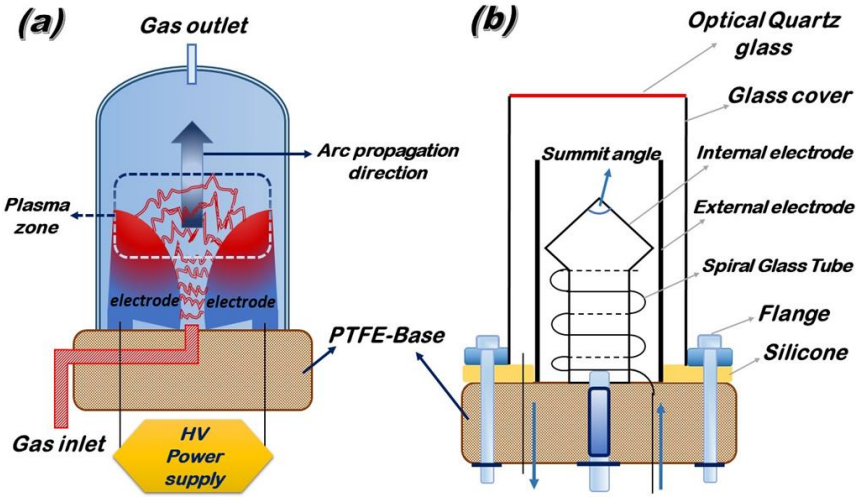

Fig. 6. Diagram of (a) gliding arc (GA) reactor and (b) rotating gliding arc (RGA) reactor for H_2 generation, depicting electrode arc propagation in the plasma zone (a) with HV supply, gas inlet/outlet, and PTFE base [122,129].

2.3. Electromagnetic Field-Driven Plasmas

2.3.1. Microwave (MW) Plasma

Microwave (MW) plasma is also known as a warm plasma with properties comparable to the characteristics of thermal plasmas. The energy dissipation in MW plasma surpasses that observed in other plasma reactors due to the high MW frequency (300 *MHz* to 10 *GHz*) [133]. The MW discharges show advantages such as high conversion, good product selectivity, and large gas treatment volume. Furthermore, the microwave discharge is an electrode free process, yielding

relatively pure plasma by avoiding electrode-induced reactions. **Fig. 7** presents a schematic diagram of a typical microwave plasma system [134]. Typically, MW discharge systems operate at either 2.45 GHz or 915 MHz and comprise several essential components, including a magnetron head, a circulator, a stub tuner, a waveguide, a plasma discharge tube, and a post-discharge chamber [134,135]. In this setup, the microwaves are created by a magnetron, and these microwaves are then guided by a waveguide to the process chamber. A dielectric tube is included within the waveguide and commonly made of quartz tube due to its transparency to microwave radiation. Consequently, when the processing gas inside the dielectric tube intersects with a waveguide, the electrons of the gas absorb the MW energy, thus igniting the ionization reactions [136]. The power can be concentrated into a confined region, where the interaction between the waveguide and the dielectric tube occurs, resulting in the formation of MW plasma, characterized by a high ion density of $>10^{11}$ cm $^{-3}$. Furthermore, depending on the level of MW power consumption, the bulk gas temperature can range from room temperature to several thousand kelvin [137]. MW plasma has various discharge modes, including surface wave discharge, electron cyclotron resonance, cavity-induced discharges, and freely expanding atmospheric plasma discharge torches [138]. However, the intricate equipment setup in MW discharges adds to considerable project costs [139].

Microwave (MW) discharges have demonstrated high conversions, high H_2 selectivity, and high gas volume treatment capacity, leading to a H_2 yield of 50-100%. MW plasma systems are electrode-free, which effectively circumvents electrode contamination and soot formation issues. The energy efficiency of microwave plasmas in hydrogen production (24−47%) is comparable to atmospheric pressure plasma jets, spark discharges, and atmospheric pressure glow discharges. To that end, many studies highlighted the potential of atmospheric pressure microwave plasma for hydrogen production [30,31,140,141]. In early studies, microwave liquid plasma was proposed for the decomposition of methane hydrate in subsea sites for hydrogen production [142]. More recently, Wang *et al.* [143] made significant advancements by developing this innovative microwave liquid discharge approach for plasma-assisted SMR. plasma-assisted SMR can occur directly in liquid water, effectively avoiding discharge instabilities due to carbon deposition. This development offers a practical and viable alternative, particularly for processing the multiphasic mixture of gaseous CH_4 and liquid H_2O, without the need of vaporizing H_2O for the reaction [143].

The primary benefits of microwave discharges include their ease of igniting plasma, flexibility in operating pressure, capacity to process large volume of gases, and the avoidance of gas phase contamination from electrode erosion debris [144].

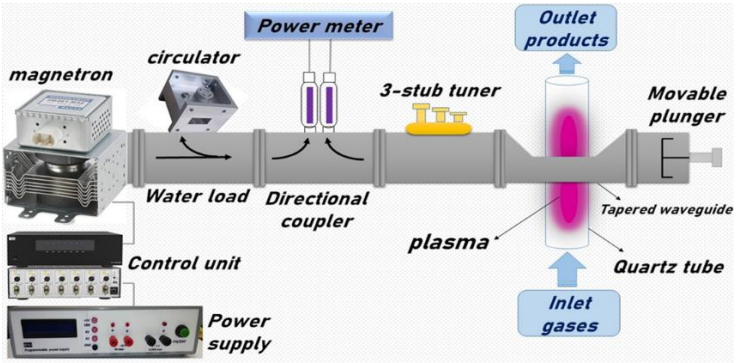

Fig. 7. Representation of a microwave plasma setup for hydrogen production, showing waveguide-based power delivery to sustain plasma within a quartz tube reactor, enabling gas inlet and product outlet for reforming processes.

2.3.2. Radio Frequency (RF) Plasma

As early as 1956, however, the Soviet physicist Veksler (1956) pointed out that the force exerted on a plasma by a radio-frequency electromagnetic field could be quite substantial, and he suggested that a suitable RF field configuration might be capable of simultaneously confining a plasma and accelerating it. The following year, Knox (1957) independently proposed that the RF fields which can be set up in a spherical resonant cavity should be used to confine a thermonuclear plasma. In the years immediately following this, a number of theoretical physicists in the Soviet Union, Britain, and America explored these possibilities in some detail [145].

An RF plasma torch consists of an induction (electromagnetic) coil and an insulation tube. An oscillating current in the induction coil produces an alternative magnetic field, which results in eddy currents producing heat via Joule heating. The key advantage of the RF plasma torch is an electrode-less design that hence avoids degradation or corrosion. However, unlike the DC plasma torch, the maximum temperature obtainable is 10000 K at a smaller plasma jet velocity [146]. RF discharges usually operate in the 1–100 MHz frequency range, resulting in a corresponding wavelength (300–3 m) much larger than the plasma reactor dimensions. The power coupling can be done through capacitive or inductive coupling, resulting in capacitively coupled plasma (CCP) and inductively coupled plasma (ICP). These kinds of discharges are mainly applied to thin-film deposition, plasma etching, the sputtering of materials and as an ion source in mass spectrometry [147]. RF power is applied to plasma reactors via either inductive or capacitive coupling as in **Figs. 8a-b**. An impedance matching unit/matching box as one important component, is connected in the circuit with the external RF generator and the reactor for stable plasma operation and reduced power loss [148].

Longmier *et al.* investigated hydrogen production from methane using a 13.56 MHz RF helicon plasma reaction chamber operating under total non-ambipolar flow conditions. The high-density non-thermal plasma ($>10^{13}$ cm^{-3}) promoted extensive methane dissociation, while ion confinement and recirculation within the reactor enhanced the probability of repeated ionization and decomposition events. At an RF power of 1300 *W* and a methane flow rate of 8 SCCM, the system achieved a methane conversion efficiency of 99.99 ± 0.06%, producing high-purity hydrogen and solid graphite as the main products. Although the process was less energy-efficient than conventional steam methane reforming, it offered the significant advantage of generating solid carbon instead of CO_2 emissions, demonstrating the potential of RF helicon plasmas for environmentally friendly hydrogen production [149].

radio frequency (RF) plasma irradiation could easily be used to generate plasma in water under high pressure [150] with the energy consumption required to produce hydrogen, oxygen, and hydrogen peroxide from water under atmospheric pressure being 0.4% of the 150 *W* of radio frequency input power [33].

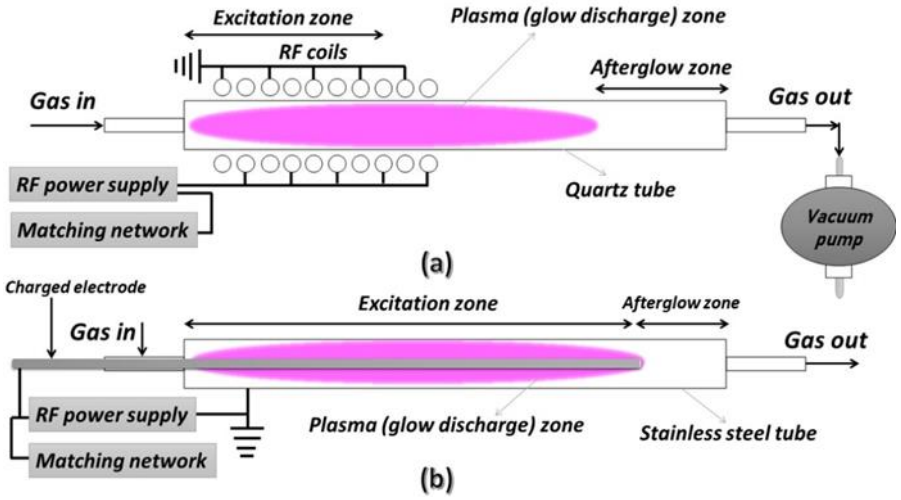

Fig. 8. Depiction of RF plasma systems for hydrogen production, illustrating (a) inductive coupling via coils in a quartz tube and (b) capacitive coupling with a charged electrode in a stainless-steel tube, each featuring excitation, glow discharge, and afterglow zones with gas flow, RF supply, matching network, and vacuum assistance [148].

3. Plasma-Catalytic Synergy and Mechanisms

The most significant challenge in plasma catalysis is understanding the underlying mechanisms and contributions from the plasma, catalysts, or combination. Plasma−catalytic interactions give rise to a range of effects, such as electrical field enhancements, alteration of the plasma discharge mode, and the formation of micro discharges within porous materials, among others. Hence, the cumulative impact of these effects adds greater complexity to the system, making the design process notably challenging [4]. the interactions between plasmas and catalysts are complicated, where catalysts affect the properties of the plasma and vice versa [151]. On one hand, packing materials change the plasma discharge properties, including the creation of micro discharges inside pores larger than the Debye length, propagation of streamers on the surface, modifications in the discharge volume, and enhancement in the electric field. These effects have a direct impact on the electron energy distribution and rates of electron-impact collisions, consequently leading to changes in the distribution of chemical species within the plasma [152]. Alternatively, plasma may also improve the catalyst properties (e.g., surface area, oxidation−reduction state, defects, and electron extraction potential) [153-157]. Additionally, micro discharges near high-curvature regions can create hot spots on the material surface [158]. More importantly, reactive species, like radicals, and excited molecules may lower activation barriers for surface reactions, providing additional pathways for yielding desired products [152]. The synergy between the plasma and included catalyst can address many of the limitations from processes with plasma alone (e.g., low H_2 selectivity). For example, zeolites [159-163], γ-Al_2O_3 [164] and Ni and Mn-based catalysts [35] facilitate the H_2 production via plasma-assisted surface reactions. The exceptional synergy between plasma and catalysts has led to innovative approaches to hydrogen production [4].

Additionally, the catalyst surface adsorption−desorption processes significantly increased H radical amount and H_2 consumption rate near the catalyst surface. This study highlighted that the catalyst could affect the spatial distributions of active species, thereby influencing the plasma chemistry indirectly [165].

DBD plasma has been mostly used for many plasma-catalysis studies [100]. Combining the DBD plasma with a catalyst can be accomplished in two general ways: (I) in-plasma catalysis (IPC) or single-stage catalysis, where the catalyst is located in the plasma zone, and (II) postplasma catalysis (PPC) or two-stage catalysis, where the catalyst is located downstream of the plasma zone [166]. For PPC operation, only long-lived plasma species or stable reaction intermediates are likely to interact (e.g., adsorb) with the catalyst surface. For IPC operation, short-lived species such as ions, radicals, and electronic and vibrationally excited species can interact with the catalyst surface, enabling alternative pathways for chemical transformations [166].

To improve CH_4 activation and H_2 selectivity, Indarto [167] investigated a DBD reactor with either Zn or Cr oxide catalysts. Remarkably, the CH_4 conversion of the plasma catalytic process was∼50% when compared to the noncatalytic process, and the addition of the catalyst increased H_2 selectivity to 40% [167]. Although no quantification of the carbon deposition was reported in this study, carbon was collected on the reactor wall and over the surface of inner electrodes, leading to catalyst and reactor deactivation in the process.

Khalifeh *et al.* [168] evaluated the decomposition of CH_4 to H_2 in a nanosecond pulsed DBD plasma reactor using three different scenarios: plasma-only, plasma with packing material (glass beads), and plasma with catalyst ($Pt–Re/Al_2O_3$). The results show that for CH_4 flow rates of 20 $mL.min^{-1}$ (or residence times of 9.46 s) and lower, CH_4 conversion increases in the order of plasma + packing > plasma + catalyst > plasma alone. At a higher flow rate of 30 $mL.min^{-1}$ (or residence time of 8.28 s), the plasma-catalytic reaction dominates with a higher CH4 conversion in the order of plasma + catalyst > plasma + packing > plasma alone. Further increasing the flow rate to 40 $mL.min^{-1}$(7.36 s) disrupts the operation of the plasma discharge and no CH_4 conversion is observed. In terms of H_2 production, for a CH_4 flow rate of 20 $mL.min^{-1}$(9.46 s), the highest production rates are achieved in the packed plasma system (0.891 *mmol/min*). However, for a CH^4 flow rate of 30 $mL.min^{-1}$, the catalytic plasma system exhibits higher H_2 production rates (1.213 *mmol/min*).

A two-stage plasma-catalytic reactor using a Ni-modified H-ZSM-5 catalyst was reported by Li *et al.* to improve aromatic yields; however, catalysts located downstream from the pulsed spark discharge plasma zone negatively affected the aromatic and H_2 yields. In the absence of catalysts (623K), a H_2 Yield of 62.6% was achieved. Conversely, with Ni/H-ZSM-5, the yield decreased by ∼15−20%. The reduction in H_2 selectivity with Ni catalysts was due to the hydrogenolysis capability of the Ni metal. Furthermore, an increase in the H_2 yield was observed with higher reaction temperatures (> 673 K) using the Ni-based catalysts, but coke yields increased significantly as well [169].

Kasinathan *et al.* investigated the influence of particle size of MgO/Al_2O_3 catalysts over CH_4 activation in a dielectric barrier discharge reactor. An increase in the conversion of CH_4 (9.5−23.0%) was observed with decreasing particle size (1.75− 0.25 mm). A similar trend was observed for H_2 production, where H_2 yields increased with decreasing particle size. The authors attributed this enhancement in the activity over smaller catalyst particles to the improved interaction between the surface of the catalyst and reaction species, highlighting the role of catalyst particle size in the conversion of CH_4 to H_2 [170].

Gas feed composition and flow rate are two common parameters often varied in plasma catalysis studies. Shuanghui *et al.* studied the influence of the CH_4 flow rate in a gliding arc plasma reaction for C_2 and H_2 production. It was found that as the CH_4 gas flow rate increased, the CH_4 conversion as well as the H_2 yield decreased, where a decrease from 81.28% to 59.66%

was observed within the range of 14−66 $mL.min^{-1}$. The authors suggested that a decrease in the residence time reduces the time for methyl radicals and H radicals to generate C_2 hydrocarbons and H_2 [171].

Ghanbari *et al.* investigated the effect of applied voltage for the conversion of CH_4 over Ni−K_2O/Al_2O_3 in a nanosecond pulsed DBD plasma reactor. The presence of the Ni−K_2O/Al_2O_3 catalyst with an applied voltage of 8 kV increased the CH_4 conversion from 76.4% to 79.3% and the H_2 production from 64.1% to 73.9%, when compared to the plasma-only system (i.e., no catalyst present). In addition, for an applied voltage of 8 kV, the presence of Ni−K_2O/Al_2O_3 reduced the required discharge power from 162 to 141.4 *W*, corresponding to a 10% reduction while also increasing the energy efficiency of the process [172].

Plasma catalysis is an alternative that holds the potential to address on demand hydrogen production while either mitigating or significantly reducing greenhouse gas (GHG) emissions, particularly when integrated with other renewable energy sources such as photovoltaics and wind power. As a result, its applicability extends to various mobile and stationary applications, including eco-friendly electricity generation with fuel cells, as well as diverse chemical uses such as food hydrogenation, metallurgical processes, and supplying the semiconductor industry with hydrogen. Plasma catalysis presents a competitive or relatively lower capital cost than conventional reforming methods, owing to its ability to address energy-intensive storage/transportation-related issues, small scale and distributed installations, and its further advantage of being compatible with various feedstocks for establishing efficient on-board hydrogen production systems [173].

However, certain challenges still affect the plasma-catalysis processes for hydrogen generation. One notable concern is the energy efficiency of the system. Broadly speaking, energy efficiency is the ratio of the energy accumulated in the product gas to the energy cost of producing the gas [174]. The reported energy efficiency for plasma-assisted hydrocarbon reforming is still well below the required threshold for commercial application. For instance, the highest reported energy efficiency for plasma-assisted steam reforming is 60% at a methane conversion of 74% [175]. The conversions of hydrocarbons, such as methane, with a DBD plasma in other reforming processes have been reported at even lower energy efficiencies. However, coupling the DBD plasma with a catalyst significantly increases the energy efficiency [176]. Much earlier studies conducted in a ferroelectric pellet packed-bed reactor showed that the energy efficiency of hydrogen production from water was 10-fold higher compared to photocatalysis, although it fell short in comparison with the electrolysis process [177]. The plasma source employed can also influence the energy efficiency of the system. For example, microwave plasma has been demonstrated to have the highest energy efficiency for CO_2 conversion at moderate pressures [178]. Additionally, due to the much higher reduced electric fields, DBD plasma has been reported to facilitate electronic excitation and bond dissociation, which are less energetically favorable pathways. Appropriate catalyst identification for plasma-driven processes can improve energy efficiency by (I) improvement of the process selectivity and moles of desired product at a specific energy input or (II) packed-bed polarization, which enhances the electric fields around the catalyst [179].

One significant advantage of plasma-catalytic systems is the capability to integrate plasma generation with renewable energy systems, offering a sustainable approach to both plasma generation and utilization. In this scenario, the electricity necessary to fuel the plasma could be derived from various renewable sources such as wind and solar, as well as emerging systems like hydro, wave, and tidal power [179].

Table 1. General comparison of plasma-assisted hydrogen production technologies with respect to plasma characteristics, hydrogen yield, energy efficiency, and practical applicability.

Method	Plasma Type	Main Energy Source	Typical Operating Conditions	Reported H_2 Yield / Conversion	Energy Efficiency	Main Advantages	Main Limitations
LIP	Laser-induced plasma	Pulsed laser irradiation	Localized plasma generated by laser ablation; atmospheric or controlled atmosphere	Qualitative hydrogen generation reported from hydrocarbon decomposition	Not explicitly reported	Precise energy deposition, catalyst-assisted reactions, nanoparticle generation, controllable plasma chemistry	High laser cost, methane dissociation limited without catalysts, scalability challenges
SD-LIP	Hybrid warm plasma	Spark discharge + laser	Laser-triggered spark discharge with catalyst assistance	Enhanced methane and propane conversion; improved H_2 production compared with conventional plasma methods	Reduced energy consumption relative to SD alone	Lower breakdown voltage, higher electron density, coke removal, catalyst self-cleaning, improved controllability	Requires laser system; industrial-scale efficiency still requires improvement
DBD	Non-thermal (cold plasma)	High-voltage AC/pulsed power	Atmospheric pressure, low temperature, kHz–MHz operation	H_2 yield typically 30–40%	6–10%	Simple design, low operating temperature, easy catalyst integration, easy scale-up, versatile feedstocks	Relatively low energy efficiency and conversion
Corona Discharge	Non-thermal (cold plasma)	High-voltage AC/DC/pulsed DC	Atmospheric pressure; non-uniform electric field near sharp electrodes	Typical H_2 yield ~56%; up to 70% reported in DRM	Typical ~10.7%; up to 14.3% reported	Simple reactor design, atmospheric-pressure operation, relatively high H_2 yield in DRM	Small plasma volume, performance strongly depends on discharge polarity
GA/RGA	Warm plasma	AC or DC arc discharge	Atmospheric pressure; gliding or rotating arc sustained by gas flow	CH_4 conversion up to 58.5%; H_2 yield up to 20.7% reported	Relatively high (qualitative)	High gas throughput, higher energy efficiency than many non-thermal plasmas, improved residence time in RGA	Electrode deterioration, carbon deposition, short residence time in conventional GA
MW Plasma	Warm plasma	Microwave radiation (typically 2.45 GHz or 915 MHz)	Electrode-free discharge; atmospheric or reduced pressure	H_2 yield 50–100%	24–47%	High conversion, high selectivity, large treatment volume, no electrode contamination, uniform energy deposition	Complex equipment and relatively high capital cost
RF Plasma	Warm/non-equilibrium plasma	Radio-frequency electromagnetic field (1–100 MHz)	Capacitive or inductive coupling; electrode-less operation possible	CH_4 conversion 99.99 ± 0.06% reported in helicon plasma reactor	Not directly reported in article	Uniform large-volume plasma, electrode-less design, low gas temperature, solid carbon co-product instead of CO_2	Lower energy efficiency than conventional SMR; complex RF power system
Plasma Catalysis	Hybrid plasma–catalyst system (commonly DBD-based)	Electrical discharge + catalyst	In-plasma catalysis (IPC) or post-plasma catalysis (PPC)	Significant improvement in CH_4 conversion and H_2 selectivity compared with plasma alone	Generally higher than plasma-only systems; catalyst reduced power demand by ~10% in reported study	Enhanced selectivity, lower activation barriers, improved energy efficiency, compatibility with renewable electricity	Mechanisms remain complex; catalyst deactivation and energy efficiency remain challenges

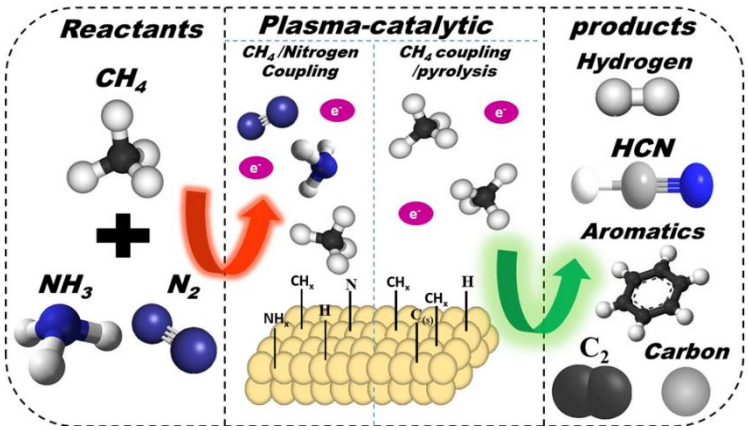

Fig. 9. Representation of a plasma-catalytic process for hydrogen production from CH_4, NH_3, and N_2, illustrating reactant coupling and pyrolysis on a catalyst surface with electron involvement, yielding H_2, HCN, aromatics, C_2, and carbon as products [3].

4. Conclusion

Despite the remarkable progress achieved in plasma-assisted hydrogen generation, several challenges still limit the large-scale implementation of these technologies. One of the most important issues is the relatively low energy efficiency of many plasma systems compared with conventional industrial processes. In addition, reactor optimization remains a critical task because plasma characteristics strongly depend on parameters such as power input, gas composition, pressure, reactor geometry, and catalyst configuration. Carbon deposition and catalyst deactivation are also significant concerns, particularly during the non-oxidative conversion of hydrocarbons, where coke formation can reduce reactor performance and operational stability over time.

Recent developments demonstrate that hybrid approaches can help overcome some of these limitations. In particular, the integration of plasma with catalysts has shown considerable potential for improving reactant conversion, hydrogen selectivity, and overall process efficiency. Similarly, advanced plasma configurations such as spark discharge-assisted laser-induced plasma (SD-LIP) offer promising solutions for suppressing coke formation, lowering breakdown voltage, and enhancing plasma controllability. Electrode-free systems, including microwave and radio-frequency plasmas, further provide attractive alternatives by eliminating electrode erosion and contamination issues.

Future research should focus on improving energy efficiency, understanding plasma–catalyst interactions, developing durable catalyst materials, and designing scalable reactor systems suitable for industrial operation. The increasing availability of renewable electricity also creates new opportunities for coupling plasma technologies with sustainable energy sources. With continued advances in reactor engineering, plasma diagnostics, and catalyst design, plasma-based hydrogen production is expected to play an increasingly important role in the transition toward clean and low-carbon energy systems.

Declaration of competing interest

The authors declare that they have no known competing financial interests or personal relationships that could have appeared to influence the work reported in this paper.

Data availability

No data is used in this article.

References

[1] M. Liao, Y. Chen, Z. Cheng, C. Wang, X. Luo, and E. Bu, Hydrogen production from partial oxidation of propane: Effect of SiC addition on Ni/Al2O3 catalyst, Appl. Energy 252 (2019) 113435.
[2] T. Ramantani, V. Evangeliou, G. Kormentzas, and D. I. Kondarides, Hydrogen production by steam reforming of propane and LPG over supported metal catalysts, Appl. Catal. B Environ. 306 (2022) 121129.
[3] J. Y. Do, R. K. Chava, N. Son, J. Kim, N. Park, D. Lee, M. W. Seo, H. Ryu, J. H. Chi, and M. Kang, Effect of Ce Doping of a Co/Al2O3 Catalyst on Hydrogen Production via Propane Steam Reforming, Catalysts 8 (2018) 413.
[4] N. Wang, H. O. Otor, G. Rivera-Castro, and J. C. Hicks, Plasma catalysis for hydrogen production: a bright future for decarbonization, ACS Catal. 14 (2024) 6749-6798.
[5] P. Bains, S. Bennett, L. Collina, E. Connelly, C. Delmastro, S. Evangelopoulou, M. Fajardy, A. Gouy, M. Kotani, J. Le Marois, and P. Levi, Global hydrogen review 2023, International Energy Agency, Paris, France, 2023.
[6] I. Dincer and C. Acar, Review and evaluation of hydrogen production methods for better sustainability, Int. J. Hydrogen Energy 40 (2014) 11094-11111.
[7] M. J. Cook, T. Nott, W. J. Trompetter, J. Futter, C. W. Bumby, and J. V. Kennedy, Plasma mediated water splitting for hydrogen production, J. Phys. Energy 7 (2025) 022002.
[8] I. Adamovich, S. D. Baalrud, A. Bogaerts, P. J. Bruggeman, M. Cappelli, V. Colombo, U. Czarnetzki, U. Ebert, J. G. Eden, P. Favia, D. B. Graves, S. Hamaguchi, G. Hieftje, M. Hori, I. D. Kaganovich, U. Kortshagen, M. J. Kushner, N. J. Mason, S. Mazouffre, S. Mededovic Thagard, H.-R. Metelmann, A. Mizuno, E. Moreau, A. B. Murphy, B. A. Niemira, G. S. Oehrlein, Z. Lj. Petrovic, L. C. Pitchford, Y.-K. Pu, S. Rauf, O. Sakai, S. Samukawa, S. Starikovskaia, J. Tennyson, K. Terashima, M. M. Turner, M. C. M. van de Sanden, and A. Vardelle, The 2017 plasma roadmap: low temperature plasma science and technology, J. Phys. D: Appl. Phys. 50 (2017) 323001.
[9] D. C. Walker and R. A. Back, Photochemistry in the Photo-Ionization Region. II. Photochemistry of Methane, Ethane, and Ethylene at Wavelengths below 900, J. Chem. Phys. 38 (1963) 1526-1535.
[10] E. M. Magee, Photolysis of Methane by Vacuum-Ultraviolet Light, J. Chem. Phys. 39 (1963) 855-858.
[11] A. R. Derk, H. H. Funke, and J. L. Falconer, Methane conversion to higher hydrocarbons by UV irradiation, Ind. Eng. Chem. Res. 47 (2008) 6568-6572.
[12] C. M. Kalamaras and A. M. Efstathiou, Hydrogen Production Technologies: Current State and Future Developments, Conf. Pap. Energy (2013) 1-9.
[13] Z. Ghorbani, P. Parvin, A. Reyhani, S. Z. Mortazavi, A. Moosakhani, M. Maleki, and S. Kiani, Methane decomposition using metal-assisted nanosecond laser induced plasma at atmospheric pressure, J. Phys. Chem. C 118 (2014) 29822-29835.
[14] M. Habibpour, P. Parvin, and R. Amrollahi, Gold fineness measurement using single-shot spark assisted laser-induced breakdown spectroscopy, Appl. Opt. 60 (2021) 1099.
[15] A. Moosakhani, P. Parvin, A. Reyhani, and S. Z. Mortazavi, Propane decomposition and conversion into other hydrocarbons using metal target assisted laser induced plasma, Phys. Plasmas 24 (2017) 013505.
[16] F. Ahmadinouri and P. Parvin, Methane conversion using spark discharge-assisted laser-induced plasma (SD-LIP) with Pd catalyst: non-oxidative hydrogen production, Chem. Eng. J. 484 (2024) 149645.
[17] F. Ahmadinouri and P. Parvin, Non-oxidative conversion of propane by employing laser-triggered spark discharge: effective hydrogen production, Energy Convers. Manage. 347 (2026) 120555.
[18] F. Ahmadinouri, P. Parvin, R. Hosseini, Z. Zare, and A. R. Rabbani, Effective methane decomposition using spark discharge assisted laser-induced plasma: an approach based on Fourier transform infrared (FTIR) spectroscopy, Spectrochim. Acta Part A Mol. Biomol. Spectrosc. 326 (2025) 125257.
[19] F. Ghasemi, P. Parvin, J. Reif, S. Abachi, M. R. Mohebbifar, and M. R. Razzaghi, Laser induced breakdown spectroscopy for the diagnosis of several malignant tissue samples, J. Laser Appl. 29 (2017) 042005.
[20] A. Moosakhani, P. Parvin, S. Z. Mortazavi, A. Reyhani, and S. Abachi, Effect of hydrocarbon molecular decomposition on palladium-assisted laser-induced plasma ablation, Appl. Opt. 56 (2017) 11.
[21] P. Parvin, H. R. Dehghanpour, M. M. Faani, A. Bavali, F. Ahmadinouri, and S. Ebrahimnasab, LIF/LIB spectroscopy of crude oil-saturated carbonate bedrock, Phys. Scr. 98 (2023) 105410.
[22] P. Mohammadimatin, P. Parvin, A. Jafargohli, A. Jahanbakhshi, F. Ahmadinouri, A. Tabibkhooei, O. Heidari, and S. Salarinejad, Signal enhancement in spark-assisted laser-induced breakdown spectroscopy for discrimination of glioblastoma and oligodendroglioma lesions, Biomed. Opt. Express 14 (2023) 5795-5816.
[23] J. S. Chang, P. A. Lawless, and T. Yamamoto, Corona discharge processes, IEEE Trans. Plasma Sci. 19 (1991) 1152-1166.
[24] B. Eliasson and U. Kogelschatz, Non equilibrium volume plasma chemical processing, IEEE Trans. Plasma Sci. 19 (1991) 1063-1077.
[25] J.-J. Zou, Y.-P. Zhang, and C.-J. Liu, Hydrogen production from dimethyl ether using corona discharge plasma, J. Power Sources 163 (2007) 653-657.
[26] C. Tendero, C. Tixier, P. Tristant, J. Desmaison, and P. Leprince, Atmospheric pressure plasmas: A review, Spectrochim. Acta Part B 61 (2006) 2-30.
[27] M. Jasiński, M. Dors, and J. Mizeraczyk, Production of hydrogen via methane reforming using atmospheric pressure microwave plasma, J. Power Sources 181 (2008) 41-45.
[28] M. Jasiński, M. Dors, and J. Mizeraczyk, Application of atmospheric pressure microwave plasma source for production of hydrogen via methane reforming, Eur. Phys. J. D 54 (2009) 179-183.
[29] M. Jasiński, M. Dors, H. Nowakowska, G. V. Nichipor, and J. Mizeraczyk, Production of hydrogen via conversion of hydrocarbons using a microwave plasma, J. Phys. D: Appl. Phys. 44 (2011) 194002.
[30] M. Jasiński, D. Czylkowski, B. Hrycak, M. Dors, and J. Mizeraczyk, Atmospheric pressure microwave plasma source for hydrogen production, Int. J. Hydrogen Energy 38 (2013) 11473-11483.

[31] D. Czylkowski, B. Hrycak, M. Jasiński, M. Dors, and J. Mizeraczyk, Microwave plasma-based method of hydrogen production via combined steam reforming of methane, Energy 113 (2016) 653-661.
[32] M. A. Lieberman and A. J. Lichtenberg, Principles of Plasma Discharges and Materials Processing, MRS Bull. 30 (2005) 899-901.
[33] A. E. E. Putra, S. Nomura, S. Mukasa, and H. Toyota, Hydrogen production by radio frequency plasma stimulation in methane hydrate at atmospheric pressure, Int. J. Hydrogen Energy 37 (2012) 16000-16005.
[34] U. Kogelschatz, Dielectric-barrier discharge: Their history, discharge physics, and industrial applications, Plasma Chem. Plasma Process. 23 (2003) 1-46.
[35] Y. Zeng, X. Zhu, D. Mei, B. Ashford, and X. Tu, Plasma-catalytic dry reforming of methane over γ-Al2O3 supported metal catalysts, Catal. Today 256 (2015) 80-87.
[36] A. Czernichowski, Gliding arc: Application to engineering and environmental control, Pure Appl. Chem. 66 (1994) 1301-1310.
[37] C. S. Kalra, Y. I. Cho, A. Gutsol, A. Fridman, and T. S. Rufael, Gliding arc in tornado using a reverse vortex flow, Rev. Sci. Instrum. 76 (2005) 025110.
[38] S. P. Gangoli, Experimental and modeling study of warm plasmas and their applications, Ph.D. dissertation, Drexel University, Philadelphia, PA, 2007.
[39] C. S. Kalra, A. F. Gutsol, and A. A. Fridman, Gliding arc discharges as a source of intermediate plasma for methane partial oxidation, IEEE Trans. Plasma Sci. 33 (2005) 32-41.
[40] I. Rusu and J. M. Cormier, On a possible mechanism of the methane steam reforming in a gliding arc reactor, Chem. Eng. J. 91 (2003) 23-31.
[41] D. H. Lee, K. T. Kim, M. S. Cha, and Y. H. Song, Plasma-controlled chemistry in plasma reforming of methane, Int. J. Hydrogen Energy 35 (2010) 10967-10976.
[42] H. Nazir, N. Muthuswamy, C. Louis, S. Jose, J. Prakash, M. E. M. Buan, C. Flox, S. Chavan, X. Shi, P. Kauranen, T. Kallio, G. Maia, K. Tammeveski, N. Lymperopoulos, E. Carcadea, E. Veziroglu, A. Iranzo, and A. M. Kannan, Is the H2 Economy Realizable in the Foreseeable Future? Part I: H2 Production Methods, Int. J. Hydrogen Energy 45 (2020) 13777-13788.
[43] W. G. Mixter, ART. VIII.–on Electrosynthesis: Carbonic Oxide and Oxygen. Methane and Oxygen. Ethylene and Oxygen. Acetylene and Oxygen. Ethane and Oxygen. Molecular Changes, Am. J. Sci. 4 (1897) 51.
[44] H. M. Mott-Smith, History of "Plasmas", Nature 233 (1971) 219.
[45] Y. Xu, X. Bao, and L. Lin, Direct conversion of methane under nonoxidative conditions, J. Catal. 216 (2003) 386-395.
[46] S. Z. Mortazavi, P. Parvin, A. Reyhani, and S. Mirershadi, Hydrogen storage property of laser induced Pd nanoparticle decorated multi-walled carbon nanotubes, RSC Adv. 3 (2013) 1397.
[47] M. Mehrabi, P. Parvin, A. Reyhani, and S. Z. Mortazavi, Hybrid laser ablation and chemical reduction to synthesize Ni/Pd nanoparticles decorated multi-wall carbon nanotubes for effective enhancement of hydrogen storage, Int. J. Hydrogen Energy (2018) 1-11.
[48] M. Mehrabi, A. Reyhani, P. Parvin, and S. Z. Mortazavi, Surface structural alteration of multi-walled carbon nanotubes decorated by nickel nanoparticles based on laser ablation/chemical reduction methods to enhance hydrogen storage properties, Int. J. Hydrogen Energy 44 (2019) 3812-3823.
[49] J. F. Ready, Effects of High-Power Laser Radiation, Academic Press, New York, 1971, pp. 161-208.
[50] L. Radziemski and D. Cremers, A brief history of Laser-Induced Breakdown Spectroscopy: From the concept of atoms to LIBS 2012, Spectrochim. Acta Part B 87 (2013) 3-10.
[51] A. W. Miziolek, V. Palleschi, and I. Schechter, Laser-induced Breakdown Spectroscopy (LIBS): Fundamentals and Applications, Cambridge University Press, Cambridge, UK, 2006.
[52] W. Sdorra and K. Niemax, Microchim. Acta 107 (1992) 319.
[53] A. J. Ball, V. Hohreiter, and D. W. Hahn, Appl. Spectrosc. 59 (2005) 348.
[54] T. M. Khan and T. BiBi, Application of NS Pulsed Laser Ablation for Dense CdS Nanoparticles Deposition in Argon Atmosphere, SOP Trans. Appl. Phys. 1 (2014) 48-54.
[55] W. W. Stoffels, E. Stoffels, G. Ceccone, and F. Rossi, Laser-induced particle formation and coalescence in a methane discharge, J. Vac. Sci. Technol. A 17 (1999) 3385-3392.
[56] M. Stafe, A. Marcu, and N. N. Puscas, Pulsed Laser Ablation of Solids (Basics, Theory and Applications), Springer, Heidelberg, 2014.
[57] D. Bäuerle, Laser chemical processing: an overview to the 30th anniversary, Appl. Phys. A 101 (2010) 447-459.
[58] J. P. Matte, M. Lamoureux, C. Moller, R. Y. Yin, J. Delettrez, J. Virmont, and T. W. Johnston, Non-Maxwellian electron distribution and continuum X-ray emission in inverse Bremsstrahlung heated plasmas, Plasma Phys. Controlled Fusion 30 (1988) 1665-1689.
[59] D. A. Cremers and L. J. Radziemski, Handbook of Laser-Induced Breakdown Spectroscopy, John Wiley and Sons, New York, 2006.
[60] S. Z. Mortazavi, P. Parvin, A. Reyhani, A. N. Golikand, and S. Mirershadi, Effect of Laser Wavelength at IR (1064 nm) and UV (193 nm) on the Structural Formation of Palladium Nanoparticles in Deionized Water, J. Phys. Chem. C 115 (2011) 5049-5057.
[61] S. Z. Mortazavi, P. Parvin, M. R. MousaviPour, A. Reyhani, A. Moosakhani, and S. Moradkhani, Time-resolved evolution of metal plasma induced by Q-switched Nd:YAG and ArF-excimer lasers, Opt. Laser Technol. 62 (2014) 32-39.
[62] N. N. Nedialkov, S. E. Imamova, P. A. Atanasov, P. Berger, and F. Dausinger, Mechanism of ultrashort laser ablation of metals: molecular dynamics simulation, Appl. Surf. Sci. 247 (2005) 243-248.
[63] L. Juha and S. Civiš, Lasers in Chemistry, in: Encyclopedia of Applied Physics, Wiley-VCH, Weinheim, 2008, pp. 899-921.
[64] H. P. Graf, M. W. Sigrist, and F. K. Kneubühl, Helv. Phys. Acta 52 (1979) 56-60.
[65] B. A. Sayyed and P. C. Stair, J. Phys. Chem. 94 (1990) 409-414.
[66] H. B. Bebb and A. Gold, Multiphoton Ionization of Hydrogen and Rare-Gas Atoms, Phys. Rev. 143 (1966) 1-24.
[67] M. D. Perry, O. L. Landen, A. Szoke, and E. M. Campbell, Multiphoton ionization of the noble gases by an intense 10^14-W/cm^2 dye laser, Phys. Rev. A 37 (1988) 747-760.

[68] G. B. Zhao, S. John, J. J. Zhang, L. Wang, S. Muknahallipatna, J. C. Hamann, J. F. Ackerman, M. D. Argyle, and O. A. Plumb, Methane conversion in pulsed corona discharge reactors, Chem. Eng. J. 125 (2006) 67-79.
[69] A. B. Redondo, E. Troussard, and J. A. Van Bokhoven, Non-oxidative methane conversion assisted by corona discharge, Fuel Process. Technol. 104 (2012) 265-270.
[70] S. Y. Liu, D. H. Mei, Z. Shen, and X. Tu, Nonoxidative conversion of methane in a dielectric barrier discharge reactor: Prediction of reaction performance based on neural network model, J. Phys. Chem. C 118 (2014) 10686-10693.
[71] F. Saleem, J. Kennedy, U. H. Dahiru, K. Zhang, and A. Harvey, Methane conversion to H2 and higher hydrocarbons using non-thermal plasma dielectric barrier discharge reactor, Chem. Eng. Process. - Process Intensif. 142 (2019) 107557.
[72] A. Indarto, J.-W. Choi, H. Lee, and H. K. Song, Effect of additive gases on methane conversion using gliding arc discharge, Energy 31 (2006) 2986-2995.
[73] H. Sun, Non-oxidative methane conversion in diffuse, filamentary, and spark regimes of nanosecond repetitively pulsed discharge with negative polarity, Plasma Process. Polym. 16 (2019) 1-15.
[74] Y. Gao, S. Zhang, H. Sun, R. Wang, X. Tu, and T. Shao, Highly efficient conversion of methane using microsecond and nanosecond pulsed spark discharges, Appl. Energy 226 (2018) 534-545.
[75] W. Cho, Y. Baek, S. K. Moon, and Y. C. Kim, Oxidative coupling of methane with microwave and RF plasma catalytic reaction over transitional metals loaded on ZSM-5, Catal. Today 74 (2002) 207-223.
[76] M. Heintze and M. Magureanu, Methane conversion into acetylene in a microwave plasma: Optimization of the operating parameters, J. Appl. Phys. 92 (2002) 2276-2283.
[77] M. Caetano and P. Patin, Coupling and reforming of methane by means of low pressure radio-frequency plasmas, Fuel 84 (2014) 2008-2014.
[78] B. Wanten, S. Maerivoet, C. Vantomme, J. Slaets, G. Trenchev, and A. Bogaerts, Dry reforming of methane in an atmospheric pressure glow discharge: Confining the plasma to expand the performance, J. CO2 Util. 56 (2022) 101869.
[79] R. Lotfalipour, A. M. Ghorbanzadeh, and A. Mahdian, Methane conversion by repetitive nanosecond pulsed plasma, J. Phys. D: Appl. Phys. 47 (2014) 365201.
[80] X. Wang, Y. Gao, S. Zhang, H. Sun, J. Li, and T. Shao, Nanosecond pulsed plasma assisted dry reforming of CH4: The effect of plasma operating parameters, Appl. Energy 243 (2019) 132-144.
[81] A. Voloshko, J.-P. Colombier, and T. E. Itina, Comparison of laser ablation with spark discharge techniques used for nanoparticle production, Appl. Surf. Sci. 336 (2014) 143-149.
[82] A. Voloshko and T. E. Itina, Nanoparticle Formation by Laser Ablation and by Spark Discharges — Properties, Mechanisms, and Control Possibilities, in: Nanoparticles Technology, Chapter 1, 2015.
[83] A. Fridman, Plasma Chemistry, Cambridge University Press, New York, 2008.
[84] M. E. Abdel-kader, W. H. Gaber, F. A. Ebrahim, and M. A. Abd Al-Halim, Characterization of the electrical breakdown for DC discharge in Ar-He gas mixture, Vacuum 169 (2019) 108922.
[85] M. V. Belkov, V. S. Burakov, A. De Giacomo, V. V. Kiris, S. N. Raikov, and N. V. Tarasenko, Comparison of two laser-induced breakdown spectroscopy techniques for total carbon measurement in soils, Spectrochim. Acta B 64 (2009) 899-904.
[86] W. Zhou, K. Li, H. Qian, Z. Ren, and Y. Yu, Effect of voltage and capacitance in nanosecond pulse discharge enhanced laser-induced breakdown spectroscopy, Appl. Opt. 51 (2012) B42-B48.
[87] Y. Wang, Y. Jiang, X. He, Y. Chen, and R. Li, Triggered parallel discharge in laser-ablation spark-induced breakdown spectroscopy and studies on its analytical performance for aluminum and brass samples, Spectrochim. Acta B 150 (2018) 9-17.
[88] M. M. Hassanimatin, S. H. Tavassoli, Y. Nosrati, and A. Safi, A combination of electrical spark and laser-induced breakdown spectroscopy on a heated sample, Phys. Plasmas 26 (2019) 033303.
[89] D. P. Subedi, U. M. Joshi, and C. S. Wong, Dielectric Barrier Discharge (DBD) Plasmas and Their Applications, in: Plasma Science and Technology for Emerging Economies: An AAAPT Experience, Springer, 2017, pp. 693-737.
[90] K. P. Francke, R. Rudolph, and H. Miessner, Design and Operating Characteristics of a Simple and Reliable DBD Reactor for Use with Atmospheric Air, Plasma Chem. Plasma Process. 23 (2003) 47-57.
[91] J. He, X. Wen, L. Wu, H. Chen, J. Hu, and X. Hou, Dielectric Barrier Discharge Plasma for Nanomaterials: Fabrication, Modification and Analytical Applications, TrAC-Trends Anal. Chem. 156 (2022) 116715.
[92] R. Brandenburg, Corrigendum: Dielectric Barrier Discharges: Progress on Plasma Sources and on the Understanding of Regimes and Single Filaments, Plasma Sources Sci. Technol. 27 (2018) 079501.
[93] K. Ollegott, P. Wirth, C. Oberste-Beulmann, P. Awakowicz, and M. Muhler, Fundamental Properties and Applications of Dielectric Barrier Discharges in Plasma-Catalytic Processes at Atmospheric Pressure, Chem.-Ing.-Tech. 92 (2020) 1542-1558.
[94] A. Chirokov, A. Gutsol, and A. Fridman, Atmospheric Pressure Plasma of Dielectric Barrier Discharges, Pure Appl. Chem. 77 (2005) 487-495.
[95] T. N. Jukes and K. S. Choi, On the Formation of Streamwise Vortices by Plasma Vortex Generators, J. Fluid Mech. 733 (2013) 370-393.
[96] T. Von Woedtke, M. Laroussi, and M. Gherardi, Foundations of Plasmas for Medical Applications, Plasma Sources Sci. Technol. 31 (2022) 054002.
[97] W. Lu, Y. Abbas, M. F. Mustafa, C. Pan, and H. Wang, A Review on Application of Dielectric Barrier Discharge Plasma Technology on the Abatement of Volatile Organic Compounds, Front. Environ. Sci. Eng. 13 (2019) 1-19.
[98] F. Peeters and T. Butterworth, Electrical Diagnostics of Dielectric Barrier Discharges, in: Atmospheric Pressure Plasma - from Diagnostics to Applications, 2019, pp. 23-49.
[99] E. E. Kunhardt, Generation of Large-Volume, Atmospheric Pressure, Nonequilibrium Plasmas, IEEE Trans. Plasma Sci. 28 (2000) 189-200.
[100] J. Li, C. Ma, S. Zhu, F. Yu, B. Dai, and D. Yang, A Review of Recent Advances of Dielectric Barrier Discharge Plasma in Catalysis, Nanomaterials 9 (2019) 1428.
[101] D. Mei and X. Tu, Conversion of CO2 in a Cylindrical Dielectric Barrier Discharge Reactor: Effects of Plasma Processing Parameters and Reactor Design, J. CO2 Util. 19 (2017) 68-78.

[102] R. Snoeckx, Y. X. Zeng, X. Tu, and A. Bogaerts, Plasma-Based Dry Reforming: Improving the Conversion and Energy Efficiency in a Dielectric Barrier Discharge, RSC Adv. 5 (2015) 29799-29808.
[103] J. Coogan and A. Sappey, Distribution of OH within silent discharge plasma reactors, IEEE Trans. Plasma Sci. 24 (1996) 91-92.
[104] A. H. Khoja, M. Tahir, and N. A. S. Amin, Recent Developments in Non-Thermal Catalytic DBD Plasma Reactor for Dry Reforming of Methane, Energy Convers. Manag. 183 (2019) 529-560.
[105] Y. Li, G. Xu, C. Liu, B. Eliasson, and B. Xue, Co-Generation of Syngas and Higher Hydrocarbons from CO2 and CH4 Using Dielectric-Barrier Discharge: Effect of Electrode Materials, Energy Fuels 15 (2001) 299-302.
[106] D. Ray, P. M. K. Reddy, and C. Subrahmanyam, Glass Beads Packed DBD-Plasma Assisted Dry Reforming of Methane, Top. Catal. 60 (2017) 869-878.
[107] W. Wang, H. H. Kim, K. Van Laer, and A. Bogaerts, Streamer Propagation in a Packed Bed Plasma Reactor for Plasma Catalysis Applications, Chem. Eng. J. 334 (2018) 2467-2479.
[108] Z. Sheng, S. Kameshima, K. Sakata, and T. Nozaki, Plasma Enabled Dry Methane Reforming, in: Plasma Chemistry and Gas Conversion, Chapter 3, 2018.
[109] H.-H. Kim, Y. Teramoto, and A. Ogata, Time-Resolved Imaging of Positive Pulsed Corona-Induced Surface Streamers on TiO2 and γ-Al2O3-Supported Ag Catalysts, J. Phys. D: Appl. Phys. 49 (2016) 415204.
[110] Q. Wang, B. H. Yan, Y. Jin, and Y. Cheng, Investigation of Dry Reforming of Methane in a Dielectric Barrier Discharge Reactor, Plasma Chem. Plasma Process. 29 (2009) 217-228.
[111] A. Bogaerts, X. Tu, and G. Van Rooij, Plasma-Based CO2 Conversion, in: Carbon Dioxide Utilisation: Transformations, De Gruyter, 2019, pp. 585-634.
[112] A. H. Khoja, M. Tahir, and N. A. S. Amin, Dry Reforming of Methane Using Different Dielectric Materials and DBD Plasma Reactor Configurations, Energy Convers. Manag. 144 (2017) 262-274.
[113] Y. Uytdenhouwen, J. Hereijgers, T. Breugelmans, P. Cool, and A. Bogaerts, How Gas Flow Design Can Influence the Performance of a DBD Plasma Reactor for Dry Reforming of Methane, Chem. Eng. J. 405 (2021) 126618.
[114] X. Tu and J. C. Whitehead, Plasma-catalytic dry reforming of methane in an atmospheric dielectric barrier discharge: Understanding the synergistic effect at low temperature, Appl. Catal. B Environ. 125 (2012) 439-448.
[115] H. L. Chen, H. M. Lee, S. H. Chen, Y. Chao, and M. B. Chang, Review of plasma catalysis on hydrocarbon reforming for hydrogen production—Interaction, integration, and prospects, Appl. Catal. B 85 (2008) 1-9.
[116] R. Aerts, W. Somers, and A. Bogaerts, Carbon Dioxide Splitting in a Dielectric Barrier Discharge Plasma: A Combined Experimental and Computational Study, ChemSusChem 8 (2015) 702-716.
[117] B. Eliasson, M. Hirth, and U. Kogelschatz, Ozone synthesis from oxygen in dielectric barrier discharges, J. Phys. D: Appl. Phys. 20 (1987) 1421-1437.
[118] R. Snoeckx and A. Bogaerts, Plasma Technology - a Novel Solution for CO2 Conversion?, Chem. Soc. Rev. 46 (2017) 5805-5863.
[119] H. Taghvaei and M. R. Rahimpour, Upgrading of Anisole Using: In Situ Generated Hydrogen in Pin to Plate Pulsed Corona Discharge, RSC Adv. 6 (2016) 98369-98380.
[120] M. Li, G. Xu, Y. Tian, L. Chen, and H. Fu, Carbon Dioxide Reforming of Methane Using DC Corona Discharge Plasma Reaction, J. Phys. Chem. A 108 (2004) 1687-1693.
[121] M. W. Li, Y. L. Tian, and G. H. Xu, Characteristics of Carbon Dioxide Reforming of Methane via Alternating Current (AC) Corona Plasma Reactions, Energy Fuels 21 (2007) 2335-2339.
[122] J. Feng, X. Sun, Z. Li, X. Hao, M. Fan, P. Ning, and K. Li, Plasma-Assisted Reforming of Methane, Adv. Sci. 9 (2022) 1-36.
[123] A. Fridman, A. Chirokov, and A. Gutsol, Non-Thermal Atmospheric Pressure Discharges, J. Phys. D: Appl. Phys. 38 (2005) R1.
[124] S. R. Sun, H. X. Wang, D. H. Mei, X. Tu, and A. Bogaerts, CO2 Conversion in a Gliding Arc Plasma: Performance Improvement Based on Chemical Reaction Modeling, J. CO2 Util. 17 (2017) 220-234.
[125] W. Wang, D. Mei, X. Tu, and A. Bogaerts, Gliding Arc Plasma for CO2 Conversion: Better Insights by a Combined Experimental and Modelling Approach, Chem. Eng. J. 330 (2017) 11-25.
[126] F. G. M. de Medeiros, F. W. B. Lopes, and B. R. de Vasconcelos, Prospects and Technical Challenges in Hydrogen Production through Dry Reforming of Methane, Catalysts 12 (2022) 363.
[127] Z. Bo, J. Yan, X. Li, Y. Chi, and K. Cen, Plasma Assisted Dry Methane Reforming Using Gliding Arc Gas Discharge: Effect of Feed Gases Proportion, Int. J. Hydrogen Energy 33 (2008) 5545-5553.
[128] F. Zhu, H. Zhang, X. Yan, J. Yan, M. Ni, X. Li, and X. Tu, Plasma-Catalytic Reforming of CO2-Rich Biogas over Ni/γ-Al2O3 Catalysts in a Rotating Gliding Arc Reactor, Fuel 199 (2017) 430-437.
[129] N. Lu, D. Sun, Y. Xia, K. Shang, B. Wang, N. Jiang, J. Li, and Y. Wu, Dry Reforming of CH4-CO2 in AC Rotating Gliding Arc Discharge: Effect of Electrode Structure and Gas Parameters, Int. J. Hydrogen Energy 43 (2018) 13098-13109.
[130] D. K. Dinh, G. Trenchev, D. H. Lee, and A. Bogaerts, Arc Plasma Reactor Modification for Enhancing Performance of Dry Reforming of Methane, J. CO2 Util. 42 (2020) 101352.
[131] H. Kwon, T. Kim, and S. Song, Dry Reforming of Methane in a Rotating Gliding Arc Plasma: Improving Efficiency and Syngas Cost by Quenching Product Gas, J. CO2 Util. 70 (2023) 102448.
[132] A. Fridman, S. Nester, L. A. Kennedy, A. Saveliev, and O. Mutaf-Yardimci, Gliding Arc Discharge, Prog. Energy Combust. Sci. 25 (1999) 211-231.
[133] M. Birau, M. A. Krasil'nikov, M. V. Kuzelev, and A. A. Rukhadze, Nonlinear Theory of a Plasma Microwave Oscillator Using Cable Waves, J. Exp. Theor. Phys. 84 (1997) 694-702.
[134] G. Chen, V. Georgieva, T. Godfroid, R. Snyders, and M. P. Delplancke-Ogletree, Plasma Assisted Catalytic Decomposition of CO2, Appl. Catal. B Environ. 190 (2016) 115-124.

[135] Y. Kim, M. Lee, and Y. J. Kim, Selective Growth and Contact Gap Fill of Low Resistivity Si via Microwave Plasma-Enhanced CVD, Micromachines 10 (2019) 689.
[136] J. Ehlbeck, U. Schnabel, M. Polak, J. Winter, T. Von Woedtke, R. Brandenburg, T. Von Dem Hagen, and K. D. Weltmann, Low Temperature Atmospheric Pressure Plasma Sources for Microbial Decontamination, J. Phys. D: Appl. Phys. 44 (2011) 013002.
[137] H. S. Uhm, Y. C. Hong, and D. H. Shin, A Microwave Plasma Torch and Its Applications, Plasma Sources Sci. Technol. 15 (2006) S26.
[138] A. A. Zamri, M. Y. Ong, S. Nomanbhay, and P. L. Show, Microwave Plasma Technology for Sustainable Energy Production and the Electromagnetic Interaction within the Plasma System: A Review, Environ. Res. 197 (2021) 111204.
[139] J. Q. Zhang, J. S. Zhang, Y. J. Yang, and Q. Liu, Oxidative Coupling and Reforming of Methane with Carbon Dioxide Using a Pulsed Microwave Plasma under Atmospheric Pressure, Energy Fuels 17 (2003) 54-59.
[140] Y. F. Wang, C. H. Tsai, W. Y. Chang, and Y. M. Kuo, Methane Steam Reforming for Producing Hydrogen in an Atmospheric Pressure Microwave Plasma Reactor, Int. J. Hydrogen Energy 35 (2010) 135-140.
[141] B. Hrycak, J. Mizeraczyk, D. Czylkowski, M. Dors, M. Budnarowska, and M. Jasiński, Hydrogen Production by the Steam Reforming of Synthetic Biogas in Atmospheric-Pressure Microwave (915 MHz) Plasma, Sci. Rep. 13 (2023) 1-15.
[142] I. Rahim, S. Nomura, S. Mukasa, and H. Toyota, Decomposition of Methane Hydrate for Hydrogen Production Using Microwave and Radio Frequency In-Liquid Plasma Methods, Appl. Therm. Eng. 90 (2015) 120-126.
[143] Q. Wang, T. Zhu, Z. Li, X. Zhu, J. Liu, and B. Sun, Plasma Activation of Methane for Hydrogen in Microwave Liquid Discharge by Auxiliary Gases: A Way to Realize Efficient Utilization of Resources, Fuel 330 (2022) 125673.
[144] M. Scapinello, E. Delikonstantis, and G. D. Stefanidis, The Panorama of Plasma-Assisted Non-Oxidative Methane Reforming, Chem. Eng. Process. Process Intensif. 117 (2017) 120-140.
[145] H. Motz and C. J. H. Watson, The Radio-Frequency Confinement and Acceleration of Plasmas, Adv. Electron. Electron Phys. 23 (1967) 153-302.
[146] K. S. Kim and T. H. Kim, Nanofabrication by thermal plasma jets: From nanoparticles to low-dimensional nanomaterials, J. Appl. Phys. 125 (2019) 070901.
[147] H. Conrads and M. Schmidt, Plasma generation and plasma sources, Plasma Sources Sci. Technol. 9 (2000) 441-454.
[148] S. Li, P. Arun, H. van den Bogaard, T. van Raak, C. Liu, and F. Gallucci, A review of experimental approaches, trends and opportunities in plasma-based gas conversion research, Front. Chem. Sci. Eng. 19 (2025) 96.
[149] B. W. Longmier, A. D. Gallimore, and N. Hershkowitz, Hydrogen production from methane using an RF plasma source in total nonambipolar flow, Plasma Sources Sci. Technol. 21 (2012) 015007.
[150] S. Nomura, S. Mukasa, H. Toyota, H. Miyake, H. Yamashita, T. Maehara, A. Kawashima, and F. Abe, Characteristics of in-liquid plasma in water under higher pressure than atmospheric pressure, Plasma Sources Sci. Technol. 20 (2011) 034012.
[151] B. Loenders, R. Michiels, and A. Bogaerts, Is a Catalyst Always Beneficial in Plasma Catalysis? Insights from the Many Physical and Chemical Interactions, J. Energy Chem. 85 (2023) 501-533.
[152] E. C. Neyts and A. Bogaerts, Understanding Plasma Catalysis through Modelling and Simulation - A Review, J. Phys. D: Appl. Phys. 47 (2014) 224010.
[153] J. Hong, W. Chu, P. A. Chernavskii, and A. Y. Khodakov, Cobalt Species and Cobalt-Support Interaction in Glow Discharge Plasma Assisted Fischer−Tropsch Catalysts, J. Catal. 273 (2010) 9-17.
[154] R. Martínez, E. Romero, C. Guimon, and R. Bilbao, CO2 Reforming of Methane over Coprecipitated Ni-Al Catalysts Modified with Lanthanum, Appl. Catal. A Gen. 274 (2004) 139-149.
[155] K. Ostrikov, E. C. Neyts, and M. Meyyappan, Plasma Nanoscience: From Nano-Solids in Plasmas to Nano-Plasmas in Solids, Adv. Phys. 62 (2013) 113-224.
[156] Y. F. Guo, D. Q. Ye, K. F. Chen, J. C. He, and W. L. Chen, Toluene Decomposition Using a Wire-Plate Dielectric Barrier Discharge Reactor with Manganese Oxide Catalyst in Situ, J. Mol. Catal. A Chem. 245 (2006) 93-100.
[157] X. Tu, H. J. Gallon, M. V. Twigg, P. A. Gorry, and J. C. Whitehead, Dry Reforming of Methane over a Ni/Al2O3 Catalyst in a Coaxial Dielectric Barrier Discharge Reactor, J. Phys. D: Appl. Phys. 44 (2011) 274007.
[158] J. Van Durme, J. Dewulf, C. Leys, and H. Van Langenhove, Combining Non-Thermal Plasma with Heterogeneous Catalysis in Waste Gas Treatment: A Review, Appl. Catal. B Environ. 78 (2008) 324-333.
[159] B. Eliasson, C. J. Liu, and U. Kogelschatz, Direct Conversion of Methane and Carbon Dioxide to Higher Hydrocarbons Using Catalytic Dielectric-Barrier Discharges with Zeolites, Ind. Eng. Chem. Res. 39 (2000) 1221-1227.
[160] H. J. Gallon, X. Tu, and J. C. Whitehead, Effects of Reactor Packing Materials on H2 Production by CO2 Reforming of CH4 in a Dielectric Barrier Discharge, Plasma Process. Polym. 9 (2012) 90-97.
[161] K. Zhang, U. Kogelschatz, and B. Eliasson, Conversion of Greenhouse Gases to Synthesis Gas and Higher Hydrocarbons, Energy Fuels 15 (2001) 395-402.
[162] K. Zhang, B. Eliasson, and U. Kogelschatz, Direct Conversion of Greenhouse Gases to Synthesis Gas and C4 Hydrocarbons over Zeolite HY Promoted by a Dielectric-Barrier Discharge, Ind. Eng. Chem. Res. 41 (2002) 1462-1468.
[163] T. Jiang, Y. Li, C. Liu, G. Xu, B. Eliasson, and B. Xue, Plasma Methane Conversion Using Dielectric-Barrier Discharges with Zeolite A, Catal. Today 72 (2002) 229-235.
[164] D. Mei, B. Ashford, Y. L. He, and X. Tu, Plasma-Catalytic Reforming of Biogas over Supported Ni Catalysts in a Dielectric Barrier Discharge Reactor: Effect of Catalyst Supports, Plasma Process. Polym. 14 (2017) 1600076.
[165] M. Zhu, A. Zhong, D. Dai, Q. Wang, T. Shao, and K. Ostrikov, Surface-Induced Gas-Phase Redistribution Effects in Plasma-Catalytic Dry Reforming of Methane: Numerical Investigation by Fluid Modeling, J. Phys. D: Appl. Phys. 55 (2022) 355201.
[166] A. Bogaerts, X. Tu, J. C. Whitehead, G. Centi, L. Lefferts, O. Guaitella, F. Azzolina-Jury, H. Kim, A. B. Murphy, W. F. Schneider, T. Nozaki, J. C. Hicks, A. Rousseau, F. Thevenet, and A. Khacef, The 2020 Plasma Catalysis Roadmap, J. Phys. D: Appl. Phys. 53 (2020) 443001.

[167] A. Indarto, Hydrogen Production from Methane in a Dielectric Barrier Discharge Using Oxide Zinc and Chromium as Catalyst, J. Chin. Inst. Chem. Eng. 39 (2008) 23-28.
[168] O. Khalifeh, H. Taghvaei, A. Mosallanejad, M. R. Rahimpour, and A. Shariati, Extra Pure Hydrogen Production through Methane Decomposition Using Nanosecond Pulsed Plasma and Pt-Re Catalyst, Chem. Eng. J. 294 (2016) 132-145.
[169] X.-S. Li, C. Shi, K.-J. Wang, X.-L. Zhang, Y. Xu, and A.-M. Zhu, High Yield of Aromatics from CH4 in a Plasma-Followed-by-Catalyst (PFC) Reactor, AIChE J. 52 (2006) 3321-3324.
[170] P. Kasinathan, S. Park, W. C. Choi, Y. K. Hwang, J. S. Chang, and Y. K. Park, Plasma-Enhanced Methane Direct Conversion over Particle-Size Adjusted MOx/Al2O3 (M = Ti and Mg) Catalysts, Plasma Chem. Plasma Process. 34 (2014) 1317-1330.
[171] S. Hu, B. Wang, Y. Lv, and W. Yan, Conversion of Methane to C2 Hydrocarbons and Hydrogen Using a Gliding Arc Reactor, Plasma Sci. Technol. 15 (2013) 555-561.
[172] M. Ghanbari, M. Binazadeh, S. Zafarnak, H. Taghvaei, and M. R. Rahimpour, Hydrogen Production via Catalytic Pulsed Plasma Conversion of Methane: Effect of Ni−K2O/Al2O3 Loading, Applied Voltage, and Argon Flow Rate, Int. J. Hydrogen Energy 45 (2020) 13899-13910.
[173] J. D. Holladay, J. Hu, D. L. King, and Y. Wang, An Overview of Hydrogen Production Technologies, Catal. Today 139 (2009) 244-260.
[174] E. Tatarova, N. Bundaleska, J. P. Sarrette, and C. M. Ferreira, Plasmas for Environmental Issues: From Hydrogen Production to 2D Materials Assembly, Plasma Sources Sci. Technol. 23 (2014) 063002.
[175] F. Geng, V. P. Haribal, and J. C. Hicks, Non-Thermal Plasma Assisted Steam Methane Reforming for Electrically-Driven Hydrogen Production, Appl. Catal. A Gen. 647 (2022) 118903.
[176] T. Nozaki and K. Okazaki, Non-Thermal Plasma Catalysis of Methane: Principles, Energy Efficiency, and Applications, Catal. Today 211 (2013) 29-38.
[177] H. Kabashima, H. Einaga, and S. Futamura, Hydrogen Generation from Water, Methane, and Methanol with Nonthermal Plasma, IEEE Trans. Ind. Appl. 39 (2003) 340-345.
[178] S. Tiwari, A. Caiola, X. Bai, A. Lalsare, and J. Hu, Microwave Plasma-Enhanced and Microwave Heated Chemical Reactions, Plasma Chem. Plasma Process. 40 (2020) 1-23.
[179] A. Bogaerts and E. C. Neyts, Plasma Technology: An Emerging Technology for Energy Storage, ACS Energy Lett. 3 (2018) 1013-1027.